SYNTHESIS OF OPTIMAL HYBRID MEMBRANE NETWORKS FOR SEAWATER DESALINATION COUPLED WITH SALT PRODUCTION PROCESSES

A Thesis

by

VARUN MAHENDRA CHAUHAN

Submitted to the Office of Graduate and Professional Studies of
Texas A&M University
in partial fulfillment of the requirements for the degree of

MASTER OF SCIENCE

Chair of Committee,	Patrick Linke
Committee Members,	Ahmed Abdel-Wahab
	Bilal Mansoor
Head of Department,	M. Nazmul Karim

August 2016

Major Subject: Chemical Engineering

ABSTRACT

Seawater Reverse Osmosis (SWRO) has become a leading desalination technology as a result of the global increase in demand for desalinated water. Several technologies have been developed, which entail salt production, to combat brine disposal issues. Integrating these options significantly impacts the economics and overall footprints of desalination systems. In this work, a novel superstructure-based approach has been developed by building upon earlier work. The main motivation of the proposed methodology is to be able to systematically explore different membrane desalination configurations coupled with salt production technologies. All possible design options have been embedded into the proposed superstructure model, whilst deploying optimization techniques that identify economically optimal solutions. Hence, the method can explore reduced water costs by extracting value from concentrates in the desalination system in the form of salt co-products. This work is the first ever attempt to propose a superstructure-based design approach for this problem.

This work considers SWRO and Nanofiltration (NF) membranes as the primary synthesis units of the membrane desalination network. NF membranes offer higher rejections of divalent ions over monovalent ions and offer potential opportunity to selectively channel streams containing high value ions to salt production operations. Furthermore, several Salt Production Processes (SPPs) involving desalination brines have also been considered as a third category for potential synthesis units within the network.

A case study involving superstructures of multiple membrane units and SPPs is used to demonstrate the proposed method. A 100,000 m^3/day production capacity plant, using the membrane modules FilmTec SW30 and NF270 by Dow, is modelled. First of the two SPP options produces calcium carbonate through sodium carbonate softening in a solid contact clarifier. The second SPP produces sodium chloride through sequential pond evaporation and evaporative crystallization. The cost optimal membrane network designs with salt production are compared against the base case of SWRO desalination without salt production. The results indicate significant reductions in water costs if salt can be co-produced in desalination systems.

DEDICATION

To my parents, sister and Rianna.

ACKNOWLEDGEMENTS

I would like to thank my committee chair, Dr. Patrick Linke, and my committee members, Dr. Ahmed Abdel-Wahab, and Dr. Bilal Mansoor, for their guidance and support throughout the course of this research.

Dr. Linke was kind enough to let me work on this project even before I registered as a graduate student so that I could get some experience in process optimization research before I made a long term commitment to this field. Furthermore, he also deserves my gratitude for his calmness and constant reassurance whenever I made mistakes in the research. Thanks also go to Dr. Sabla Alnouri for her supervision and help, without which, this project would not have finished. I also want to extend my gratitude to my friends, colleagues and the department faculty and staff for making my time at Texas A&M University at Qatar a great experience. Finally, thanks to my family for their encouragement.

NOMENCLATURE

f	Split fraction at a splitter node
F	Mass flow rate of stream (kg/s)
X	TDS in a stream (mg/L)
y	Binary variable used to decide the existence of a membrane type
P	Pressure (bar)
PI	Initial pressure of a connection (bar)
PF	Final pressure of a connection (bar)
H	Pressure head of a connection
γ	Rejection of ions by membrane
NM	Number of module
RE	Membrane recovery
L	Plant lifetime (years)
TAC	Total Annualized Costs
TCI	Total Capital Investment
DCC	Direct Capital Costs
SC	Soft Costs
CC	Capital costs
TOC	Total Operating costs
VOC	Variable Operating Costs
FOC	Fixed Operating Costs

OC	Operating and maintenance costs
PW^{Pumps}	Power required for all the pumps in the membrane network (kW)
PW^{ERDs}	Power made by all the ERDs in the membrane network (kW)
T	Temperature (°C)
NS	Number of skids
A	Ionic feed flow into a SPP (mg/s)
β	Fraction of SPP feed that is distributed to SPP outlet streams
δ	Ionic mass fraction in salt being added or produced
$G_{s,m}^{M}$	Salt addition rate (mg/s)
$G_{s,n}^{N}$	Salt production rate (mg/s)
d_t	Fraction of SPP-2 feed that is converted to lost and recovered water
d_p	Fraction of SPP-2 feed that is lost as evaporated water
$X_{1,2}^{F-S\prime}$	SPP-2 feed concentration of calcium (mol/L)
$X_{2,2}^{F-S\prime}$	SPP-2 feed concentration of sodium (mol/L)
$S_{CaCO3\prime}$	Precipitation onset solubility of $CaCO_3$ (mol/L)
$S_{NaCl\prime}$	Precipitation onset solubility of NaCl (mo/L)
Pf_j^{NF}	NF membrane permeate flux (m/s)
L_s	Solution permeability (m/s.bar)
ΔP_m	Applied pressure difference in membrane
π_j^F	Osmotic pressure of feed
π_j^P	Osmotic pressure of permeate

ΔP	Pressure drop in membrane
$P_j^{F-RO,MAX}$	Maximum RO membrane feed pressure
$P_j^{F-NF,MAX}$	Maximum NF membrane feed pressure
$X^{PROD,MAX}$	Maximum TDS of product water
$X_i^{PROD,MAX}$	Maximum ionic concentration of product water
NM_j^{RO-MAX}	Maximum number of modules in RO membrane unit
NM_j^{RO-MIN}	Minimum number of modules in RO membrane unit
NM_j^{NF-MAX}	Maximum number of modules in NF membrane unit
NM_j^{NF-MIN}	Minimum number of modules in NF membrane unit
FEED-RO	Superscript denoting the feed splitter to RO feed connection
FEED-NF	Superscript denoting the feed splitter to NF feed connection
FEED-PROD	Superscript denoting the feed splitter to NF feed connection
PRO-RO	Superscript denoting the RO permeate to RO feed connection
PRO-NF	Superscript denoting the RO permeate to NF feed connection
PRO-PROD	Superscript denoting the RO permeate to product water connection
BRO-RO	Superscript denoting the RO brine to RO feed connection
BRO-NF	Superscript denoting the RO brine to NF feed connection
BRO-BRINE	Superscript denoting the RO brine to network brine connection
BRO-S	Superscript denoting the RO brine to SPP feed connection
PNF-PROD	Superscript denoting the NF permeate to product water connection
PNF-RO	Superscript denoting the NF permeate to RO feed connection

PNF-NF	Superscript denoting the NF permeate to NF feed connection
PNF-S	Superscript denoting the NF permeate to SPP feed connection
BNF-RO	Superscript denoting the NF brine to RO feed connection
BNF-NF	Superscript denoting the NF brine to NF feed connection
BNF-BRINE	Superscript denoting the NF brine to network brine connection
BNF-S	Superscript denoting the NF brine to SPP feed connection
S-RO	Superscript denoting the SPP brine to RO feed connection
S-NF	Superscript denoting the SPP brine to NF feed connection
S-PROD	Superscript denoting the SPP recovered water to product water connection
S-BRINE	Superscript denoting the SPP brine to network brine connection
S-LOST	Superscript denoting the SPP lost water to network lost water connection
S-S	Superscript denoting the SPP brine to SPP feed connection
F-RO	Superscript denoting the RO feed stream
P-RO	Superscript denoting the RO permeate stream
B-RO	Superscript denoting the RO brine stream
F-NF	Superscript denoting the NF feed stream
P-NF	Superscript denoting the NF permeate stream
B-NF	Superscript denoting the NF brine stream
F-S	Superscript denoting the SPP feed stream
S-Br	Superscript denoting the SPP brine stream

S-Lo	Superscript denoting the SPP lost water stream
S-Re	Superscript denoting the SPP recovered water stream
PROD	Superscript denoting the network brine stream
FEED	Superscript denoting the network feed stream
j	Subscript denoting membrane unit ‘j’
j,j’	Subscript denoting connection from membrane unit j to j’
j,s	Subscript denoting connection from membrane unit j to SPP ‘s’
s	Subscript denoting SPP ‘s’
s,j	Subscript denoting connection from SPP ‘s’ to membrane unit ‘j’
s,s’	Subscript denoting connection from SPP ‘s’ to another SPP ‘s’’
i	Subscript denoting ion ‘i’

TABLE OF CONTENTS

Page

LIST OF FIGURES

Page

LIST OF TABLES

Page

1. INTRODUCTION

Over the past 60 years, several thermal and membrane based desalination technologies have been developed and improved for the production of potable water. Some of the major desalination technologies are Multiple Effect Distillation (MED), Multi-Stage Flash (MSF) and Reverse Osmosis (RO) desalination[1]. RO has emerged as the leading desalination technology due to relatively lower energy demands, energy recovery and reduction in costs of the membranes. Currently RO accounts for 44% of the global desalinated water production and 80% of the global desalination plants. The Middle East itself accounts for 50% of the global production capacity even though it only consists of 2.9% of the global population[2]. Nanofiltration (NF) membranes have been developed for brackish water desalination as a substitute for RO membranes. Along with having rejections between those of an RO and Ultrafiltration (UF) membranes, NF membranes have higher rejection rates for divalent ions than for monovalent ions. Furthermore, NF membranes have lower energy requirements than RO membranes[2]. Such lower cost desalination systems using NF membranes have been developed and implemented[3].

A major concern with desalination technologies is brine handling. The common and most cost effective brine handling solution would be to discharge it back into the seawater, but this practice has several detrimental effects to the environment and marine life[4]. Several brine treatment processes have been proposed which focus on reducing the volume of the brine being disposed[2]. Some of these approaches include developing new technologies such as Electrodialysis, Membrane Distillation, Forward Osmosis etc.,

integrating different desalination technologies to improve recovery and recovering commercial mineral salts from the brine. The methodologies usually used for salt recovery from desalination brines include evaporation, either in an evaporation pond or a crystallizer, and softening using chemicals such as lime and soda ash [2 5].

2. BACKGROUND

2.1 Membrane network optimization

As a result of being the leading desalination technology, improvements in the RO process design through better membrane network configurations has received considerable attention in the previous three decades. The majority of this work has been through superstructure optimization. A superstructure consists of all the possible connections between all the units in the superstructure. Thus all the feasible network designs are embedded in the superstructure. The optimized design is then extracted from this superstructure subject to an objective function and process constraints[6].

The first work to perform RO network synthesis by solving for the local optimum in a rich superstructure as a Mixed Integer Non-Linear Program (MINLP) was done by El-Halwagi[7]. All the units and stream connectivity were represented using the State Space approach. A modified state-space representation was used as a non-linear program to develop membrane desalination networks by Voros et al.[8]. Similar to the work by Voros et al., Maskan et al. also use non-linear programs to develop RO membrane networks[9]. A State Space formulation was used by Zhu et al. to design flexible RO membrane networks[10]. They also developed an optimal maintenance schedule. Lu et al. modify El-Halwagi's formulation where structural variables were only used to select between different membrane types[11]. Using an exhaustive multi-objective formulation in which both technical and environmental performance was considered, Vince at al. optimize one and two unit RO membrane networks[12]. Using Genetic Algorithms, Guria et al. solve for

optimal RO membrane networks[13]. Saif el al. optimize RO networks through superstructure optimization with iterative Mixed Integer Linear Program (MILP)[14]. All the above mentioned work solve for local optimum rather than for global optimum. Using binary variables in State Space formulation and solving for global optimization, Marcovecchio et al. develop an algorithm for optimal RO membrane operating conditions for conventional membrane network designs[15]. Marriot et al. recommend a similar approach but not for SWRO designs[16]. Though using large computational times, Saif et al. perform RO membrane superstructure optimization using deterministic global optimization methods[17]. All the above mentioned work usually present results with one or two membrane networks and consider only two components, water and Total Dissolved Salts (TDS). Alnouri and Linke globally optimize RO membrane networks by initially determining the performance limit of one, two and three RO membrane superstructures and then comparing them to globally optimized leaner superstructure design classes[6]. Although this work considers only two feed components, water and salt (TDS), their next work uses a similar formulation but for a multi component feed which contains water and the major ions that are present in seawater[18]. Another work of theirs globally optimized the multi-component feed RO membrane networks while considering boron removal and different RO membranes [19]. This allowed them to study pH influences on the performance of the system.

Though literature is available that optimizes superstructures consisting different membrane types, all the membranes in such work have the same connections within the superstructure. None of the literature on membrane network optimization takes into

account different membrane types, each with a different set of connections within the superstructure. For instance, no superstructure optimization of hybrid membrane networks consisting RO and NF membranes has been attempted. Due to the characteristic behavior of NF membranes to offer higher rejections to divalent ions over monovalent ions[2], the relative differences between the concentrations of the brine and permeate streams from NF membranes can vary depending on the composition of the NF membrane feed. Meanwhile for RO membranes, the differences between the concentrations of the permeate and brine streams are always large due to their high rejections for all ions. These differences in the performance of RO and NF membranes warrant different connections within a hybrid RO-NF membrane superstructure. No current work attempts at optimizing such superstructures.

2.2 Salt production processes

Seawater consists large concentrations of several ions in varying amounts. In order to determine the profitability of producing mineral salts from seawater along with desalination, the maximum possible revenue that can be acquired by the sale of salts made of seawater ions was studied. This analysis will aid us in understanding the value of the ions in the seawater. To obtain this maximum revenue from seawater, salt production costs were not taken into consideration. The cations considered for this study are Sodium (Na^+), Magnesium (Mg^{++}), Calcium (Ca^{++}) and Potassium (K^+). The anions considered are Chloride (Cl^-), Sulfate (SO_4^{--}) and Bicarbonate (HCO_3^-). The seawater concentrations considered for this study are those of the typical seawater and Eastern Mediterranean. Their concentrations are shown in Table 1[18]. Initially bulk prices for all the salts obtainable

from the combinations of the above ions were estimated. These prices are shown in Table 2. Using these prices, the salts were arranged from most expensive to least expensive salts. The following flowchart was then used to sequentially produce the most expensive salts using all the ions from seawater.

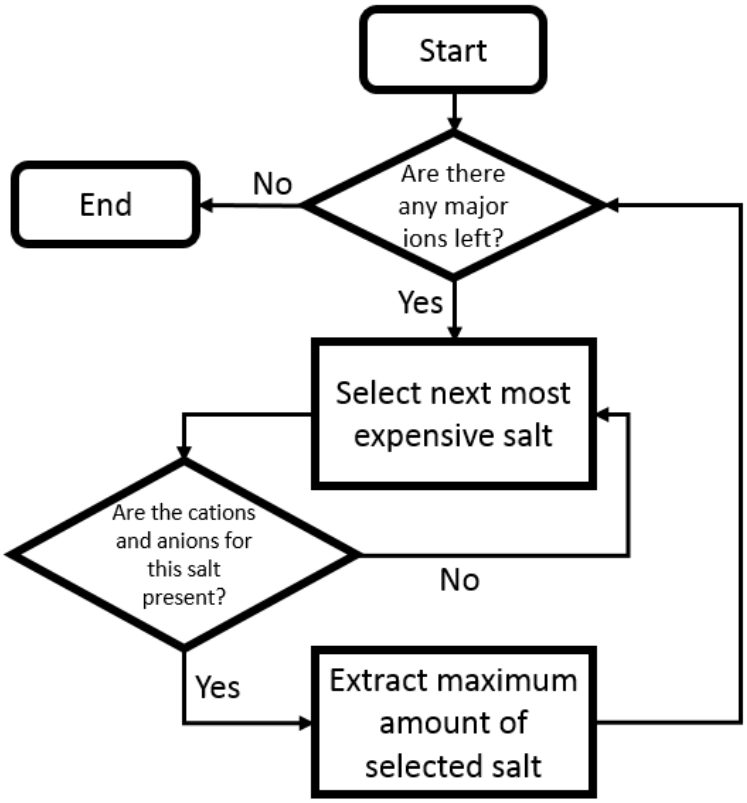

Figure 1 Flowchart for determination of maximum value of seawater salts

Table 1 Seawater compositions used for seawater salts value analysis

	Typical seawater	Eastern Mediterranean
	mg/L	mg/L
Na	10556	11800
Mg	1262	1403
Ca	400	423
K	380	463
Cl	18980	21200
HCO_3	140	0
SO_4	2649	2950
TDS	34367	38239

Table 2 Bulk prices of seawater salts

Salts	Price ($/tn)	Salts	Price ($/tn)
KOH[20]	969	$Ca(OH)_2$[21]	138
K_2CO_3[20]	860	Na_2SO4[20]	122
K_2SO_4[22]	600	KCl[20]	115
$MgSO_4$[20]	396	H_2CO_3[20]	94
$MgCO_3$[23]	329	HCl[20]	85
$NaOH$[20]	300	$NaCl$[20]	65
$MgCl$[20]	281	$CaCO_3$[20]	62
$CaCl_2$[20]	275	H_2SO_4[20]	62
$Mg(OH)_2$[20]	244	$CaSO_4$[24]	10
Na_2CO_3[20]	165		

Table 3 Maximum value obtainable from salts of seawater ions

Typical seawater		Eastern Mediterranean	
	$/m^3		$/m^3
KOH	0.53	KOH	0.64
$MgSO_4$	1.31	$MgSO_4$	1.46
NaOH	5.51	NaOH	6.16
$Mg(OH)_2$	0.25	$Mg(OH)_2$	0.27
$CaCl_2$	0.30	$CaCl_2$	0.32
H_2CO_3	0.01	H_2CO_3	0.00
HCl	1.60	HCl	1.79
Total	9.51	Total	10.65

Table 3 presents the salts, their revenue and the total maximum revenue obtainable from the ions in the three seawaters considered. It can be seen that this maximum revenue for all the three cases is approximately 10 $/m^3. Assuming the typical desalination cost to be 1 $/m^3 of produced water, this value is approximately 20 times the desalination cost. This analysis shows us that high value salts can be extracted from seawater along with desalination. The revenue from the sale of these salts can be used to offer discounts and reduce the price of the pure desalinated water sold.

In a bid to reduce the volume and quality of the desalination brines being disposed, several salt recovery methodologies from brine have been developed and implemented. Solar evaporation ponds use the Sun's energy to naturally evaporate water from the brine, hence leaving salt behind. This salt can later be processed or sent for disposal. Such ponds have relatively low construction and operation costs[25]. The use of solar ponds is suitable in arid regions. Furthermore, since shallow ponds allow for higher evaporation rates, large areas of land are also a necessity for large volumes of brine evaporation[26]. Evaporative brine crystallizers and concentrators are also used to further concentrate brine while producing salts. The three most common types of crystallizers are the forced circulation crystallizers, turbulence with Draft Tube and Baffle (DTB) crystallizer and the OSLO crystallizer[27]. Crystallizers are common in Zero-Liquid Discharge (ZLD) processes. Two pilot plant studies of ZLD processes for brackish water desalination using evaporation-crystallization with a flash evaporator were done by Zarzo et al.[28]. Mickley suggested several combinations for ZLD processes for different feed water qualities[29]. Intermediate Chemical Demineralization (ICD) causes the precipitation of mineral salts from

desalination brines using either softening chemicals or seeds of the precipitating salt itself. Gabelich et al. studied the performance of a two RO stage brackish water desalination system with a softening process between the RO stages[30]. The softening, which was done with sodium hydroxide and sodium bicarbonate in a solid contact reactor, increased the recovery of the entire process from 85% to 95%. Rahardianto et al. evaluated the intermediate calcium carbonate ($CaCO_3$) removal through calcium hydroxide dosing followed by the seeded precipitation of gypsum. They mentioned that lime induced $CaCO_3$ precipitation was able to remove antiscalants from the brine and hence improve the performance of the second stage RO for brackish water systems[31]. SAL-PROC integrates the above mentioned processes of evaporative crystallization and softening in a sequential manner to produce several salts such as gypsum ($CaSO_4$), sodium chloride (NaCl), magnesium hydroxide ($Mg(OH)_2$), calcium chloride ($CaCl_2$) and calcium hydroxide ($Ca(OH)_2$) amongst others. The process has been used for brackish water from the Tutchewop Lake in Australia[32]. Eutectic Freeze Crystallization (EFC) freezes the brine solution to its eutectic point, below which ice and salts are simultaneously produced[33]. Theoretically EFC can achieve total conversion of feed brine solution to solid products of ice and salts. Moreover, the process has lower energy needs than typical cooling or evaporative processes. At the bench scale, EFC has been used to produce magnesium sulfate heptahydrate ($MgSO_4 .H_2O$) from flue gas desulfurization stream[34]. Membrane Crystallization (MCr) uses hydrophobic membranes to transport water in the vapor phase to the distillate side of the membranes while creating supersaturation on the warm feed side. This leads to the precipitation of salts on the feed side of the membranes. Though

still operated only on a bench scale, Drioli et al. proposed flow designs of an integrated RO-NF-MCr system with softening to produce NaCl, $CaCO_3$ and $MgSO_4$[35]. Bipolar Membrane Electrodialysis (BMED) is used to separate cations and anions though a bipolar membrane under an applied potential. The cations and anions combine with the hydroxide ions and protons respectively in their chambers to produce bases and acids respectively. Badruzzaman et al. proposed the production of hydrochloric acid (HCl) and sodium hydroxide (NaOH) from a highly concentrated solution through the use of BMED along with softening and a bioreactor[36].

All the above mentioned processes can be conceptually represented as a single-input multiple-output model as shown in Figure 2.

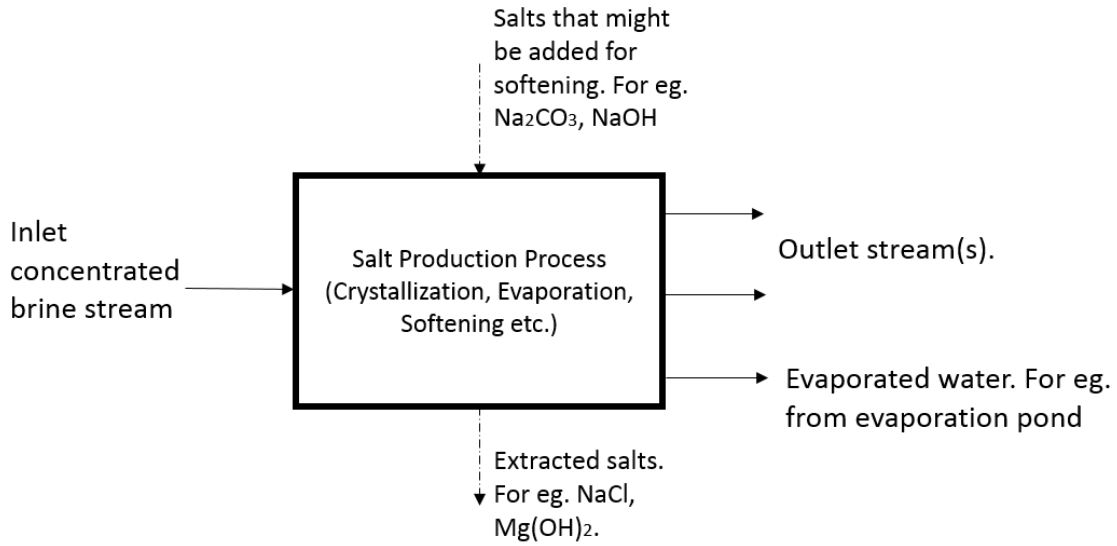

Figure 2 Conceptual representation of a salt production process

The model can have other inputs too in the form of salts for softening and energy for crystallizers, MCr etc. Furthermore, representing the processes in such a manner allows for their incorporation into a superstructure. This incorporation of salt production processes within desalination superstructures has not been done yet in any work.

3. SCOPE

As mentioned before, current literature does not account for the optimization of membrane network superstructures consisting of membranes with different types of connections such as a RO and NF hybrid membrane superstructure. Moreover, optimization work of desalination membrane networks do not yet take into consideration salt production processes.

This work deals with the superstructure optimization of membrane networks while accounting for both the above mentioned aspects. Such an approach to account for both hybrid RO-NF membranes and salt production processes will allow for the synergetic performance between the SPPs and different membrane types to be explored. Monovalent and divalent ion rich streams can be generated by NF membranes which can then be used for enhanced salt production. This enhanced salt production along with produced water will lead to lower cost designs. Such network designs cannot be obtained by conventional approaches. The conventional trial and error approach either uses SPPs to treat the final brine of the desalination system or to treat the brine of a single desalination membrane. Such an approach misses out on the usage of intermediate streams which may be of optimum composition for salt production. Therefore the major objective of this work is to develop a novel search scheme and superstructure representation that consists of different desalination membrane types and salt production technologies so as to achieve reduced water costs by extracting value from concentrates in the desalination system in the form of salt co-products. This work will be the first ever attempt to develop a superstructure-based design approach for this problem.

4. METHODOLOGY

The problem is formally stated as below.

Given

- a number of ions in seawater,
- a seawater feed stream with known flow, pressure and ionic concentrations,
- a product water production capacity and ionic concentrations,
- a number of membrane units,
- ionic rejections and cost models for RO and NF membranes,
- input-output performance and cost models for SPPs,

determine the minimal cost desalination membrane and SPP network design while taking into consideration the revenue generated from the salt. Therefore the objective function of this optimization problem is: Minimize *TAC*. Here *TAC* refers to the Total Annualized Cost. *TAC* is determined as the sum of the total annual operating costs (TOC) and the total annualized capital investment (TCI) using the following equation.

$$TAC = TCI + TOC \tag{1}$$

The total annual operating costs and annualized capital investments are determined as sums of the respective costs of the membrane network and salt production processes through the following equations.

$$TCI = TCI_{SPP} + TCI_{Membrane} \tag{2}$$

$$TOC = TOC_{SPP} + TOC_{Membrane} \tag{3}$$

The determination of the capital and operating costs of the membrane networks and SPPs is case-study specific and can be determined as a function of the system variables

that apply to that process. Such an example of a detailed cost function of a desalination and SPP system will be presented in the case study section. The following section provides the general formulation developed to model the membranes and SPPs.

Certain sets were defined to be used in the mathematical formulation of the problem.

I {i=1,2,…, Ni| I is a set of ionic species in a water stream}

J {j=1,2,…, Nm| J is a set of membrane units in the superstructure}

S {s=1,2,…, Ns| S is a set of SPPs in the superstructure}

M {m=1,2,…, Nm| M is a subset of S. It is the number of input salts for each SPP 's' in the superstructure}

N {n=1,2,…, Nn| N is a subset of S. It is the number of produced salts from each SPP 's' in the superstructure}

The developed superstructure consists of three building blocks/units: RO membrane, NF membrane and salt production process (SPP). Splitters and mixers are used to connect the streams between these three units. Splitters divide and distribute streams to different destinations while mixers receive and mix streams from different splitters to produce one exit stream[6]. Splitters are associated with the seawater feed, every membrane and SPP outlet stream. Mixers are associated with the feed streams of every membrane and SPP and network outlet streams: product water, network brine and lost water. The lost water outlet mixer receives streams of evaporated water from any SPP. The following sections describe the purpose and mathematical modelling of the three building blocks.

4.1 RO membranes

Due to its high rejections for all ions in seawater, the primary purpose of RO membranes is the desalination of its feed stream. These spiral wound membrane elements have two outputs, low concentration permeate and high concentration brine streams. Thus RO membranes are represented using a model with one input and two outputs. The input stream is characterized with flow (F_j^{F-RO}) and ionic concentrations ($X_{j,i}^{F-RO}$). The permeate and brine streams are characterized with flows (F_j^{P-RO}) and (F_j^{B-RO}) and ionic concentrations ($X_{j,i}^{P-RO}$) and ($X_{j,i}^{B-RO}$) respectively. The following equations describe the flow and component balance around a RO membrane *j*.

$$\mathrm{F_j^{F-RO}} = \mathrm{F_j^{P-RO}} + \mathrm{F_j^{B-RO}} \quad j \in J \tag{4}$$

$$F_j^{F-RO} \times X_{j,i}^{F-RO} = F_j^{B-RO} \times X_{j,i}^{B-RO} + F_j^{P-RO} \times X_{j,i}^{P-RO} \qquad j \in J, i \in I \tag{5}$$

Equation 6 determines the flow of the permeate of membrane *j* using the recovery (RE_j^{RO}) and membrane feed flow.

$$F_j^{P-RO} = RE_j^{RO} \times F_j^{F-RO} \qquad j \in J \tag{6}$$

Equation 7 determines the permeate composition based on the ionic rejections ($\gamma_{i,j}^{RO}$) of the RO membrane *j*. The ionic rejections for RO membranes can be calculated using parameters or correlations that are a function of the temperature, pressure or other operating conditions.

$$X_{i,j}^{P-RO} = X_{i,j}^{F-RO} \times (1 - \gamma_{i,j}^{RO}) \quad j \in J, i \in I \tag{7}$$

Cost models, capital and operating, for RO membranes need to be developed in order to account for the expenditure of RO membranes in the overall cost function *TAC*. An example of such RO membrane cost models is presented in the case study section.

4.2 NF membranes

NF membranes possess higher rejections for divalent ions than monovalent ions. Thus their purpose, along with desalination, is to achieve partial separation of monovalent and divalent ions. This separation can be then used to channel only monovalent or divalent ionic streams to SPPs for salt production of such ions. Different NF membranes achieve this separation to different degrees. NF membranes such as Dow FilmTec NF90 achieve high RO-like rejections for all ions with little difference in monovalent and divalent rejections. On the other hand, NF membranes such as Dow FilmTec NF270 can achieve a large difference in the monovalent and divalent ion rejections[3]. The modelling formulation presented here applies to both kinds of NF membranes. Similar to RO membranes, these spiral wound membrane elements have two outputs, low concentration permeate and high concentration brine streams and hence are represented using a model with one input and two outputs. The input stream is characterized with flow (F_j^{F-NF}) and ionic concentrations ($X_{j,i}^{F-NF}$). The permeate and brine streams are characterized with flows (F_j^{P-NF}) and (F_j^{B-NF}) and ionic concentrations (X_j^{B-NF}) and ionic concentrations ($X_{j,i}^{P-NF}$) and ($X_{j,i}^{B-NF}$) respectively. The following equations describe the flow and component balance around a NF membrane *j*.

$$F_j^{F-NF} = F_j^{P-NF} + F_j^{B-NF} \qquad j \in J \tag{8}$$

$$F_j^{F-NF} \times X_{j,i}^{F-NF} = F_j^{B-NF} \times X_{j,i}^{B-NF} + F_j^{P-NF} \times X_{j,i}^{P-NF} \qquad j \in J, i \in I \tag{9}$$

Equation 10 determines the flow of the permeate of membrane *j* using the recovery (RE_j^{NF}) and membrane feed flow.

$$F_j^{P-NF} = RE_j^{NF} \times F_j^{F-NF} \qquad j \in J \tag{10}$$

Equation 11 determines the permeate composition based on the ionic rejections ($\gamma_{i,j}^{RO}$) of the NF membrane *j*. The ionic rejections for NF membranes can be calculated using parameters or correlations that are a function of the temperature, pressure or other operating conditions.

$$X_{i,j}^{P-NF} = X_{i,j}^{F-NF} \times (1 - \gamma_{i,j}^{NF}) \qquad j \in J, i \in I \tag{11}$$

Cost models, capital and operating, for NF membranes need to be developed in order to account for the expenditure of NF membranes in the overall cost function (*TAC*). An example of such NF membrane cost models is presented in the case study section.

In the superstructure, each membrane unit can either be a RO membrane or a NF membrane. Binary variables (*y*) are used in the formulation to select each membrane type. Each membrane is assigned two binary variables (y_j^{RO} and y_j^{NF}). The following equations ensure that either RO or NF is assigned as the membrane type for membrane *j*.

$$y_j^{RO} + y_j^{NF} = 1 \qquad j \in J, y_j^{RO}, y_j^{NF} \in [0,1] \tag{12}$$

Once the membrane unit type binaries (y_j^{RO} and y_j^{NF}) have been selected, the following equations ensure that the connections for that membrane type have the same binary value.

$$y_j^{RO} = y_j^{FEED-RO} = y_{j,j\prime}^{PRO-RO} = y_{j,j\prime}^{PRO-NF} = y_{j,j\prime}^{PRO-PROD} = y_{j,j\prime}^{BRO-RO} = y_{j,j\prime}^{BRO-NF} = y_{j,j\prime}^{BRO-BRINE} = y_{j,j\prime}^{BRO-S} = y_{j\prime,j}^{PNF-RO} = y_{j\prime,j}^{PRO-RO} = y_{j\prime,j}^{BNF-RO} = y_{j\prime,j}^{BRO-RO} = y_{s,j}^{S-RO}$$

$$j, j' \in J, j \neq j', s \in S \tag{13}$$

$$y_j^{NF} = y_j^{FEED-NF} = y_{j,j'}^{PNF-RO} = y_{j,j'}^{PNF-NF} = y_{j,j'}^{PNF-PROD} = y_{j,j'}^{BNF-RO} = y_{j,j'}^{BNF-NF} = y_{j,j'}^{BNF-BRINE} = y_{j,j'}^{BNF-S} = y_{j',j}^{PNF-NF} = y_{j',j}^{PRO-NF} = y_{j',j}^{BNF-NF} = y_{j',j}^{BRO-NF} = y_{s,j}^{S-NF} = y_{j,s}^{PNF-S} \qquad j, j' \in J, j \neq j', s \in S \tag{14}$$

4.3 Salt production processes

A SPP has a single input stream with multiple outlet streams: brine, pure water or evaporated lost water. The SPP model developed in this work calculates the flow and composition of all the outlet streams and the amount of salt produced.

4.3.1 Determining SPP outlet flows

The following equations are used to determine the flows of the outlet brine stream (F_s^{S-Br}), recovered water stream (F_s^{S-Re}) and lost water stream (F_s^{S-Lo}).

$$F_s^{S-Br} = F_s^{F-S} \times \beta_s^{S-Br} \qquad s \in S \tag{15}$$

$$F_s^{S-Re} = F_s^{F-S} \times \beta_s^{S-Re} \qquad s \in S \tag{16}$$

$$F_s^{S-Lo} = F_s^{F-S} \times \beta_s^{S-Lo} \qquad s \in S \tag{17}$$

F_s^{F-S} represents the SPP feed flow and β represents the fraction of the feed flow that exits the SPP in outlet streams. β can be defined as a parameter or using a correlation that is function of the characteristic variables of that salt production technology. For instance, SPPs like crystallizers have two outlet streams, brine and distillate, and hence two β factors, β_s^{S-Br} and β_s^{S-Re}, need to be defined. β_s^{S-Lo} ,in this case, will be defined as 0 since there is no loss of water.

4.3.2 Determining salt production and outlet stream concentrations

To determine the amount of salt produced, several variables need to be defined. These variables include the amount of salt added ($G_{s,m}^{M}$), ionic concentration of recovered water ($X_{i,s}^{S-Re}$), ionic concentration of lost water ($X_{i,s}^{S-Lo}$) and the solubility of the salt being produced ($S_{n,s}^{S}$). Similar to β, these parameters can also be defined either using literature obtained parameters or through correlations that are functions of the processes variables. An SPP might have salt addition for several purposes such as pH change and softening. Salt solubility determines how saturated a solution is with respect to that salt, which then governs the amount of salt being precipitated. Different technologies achieve this supersaturation through different means such as reducing temperature, increasing concentration, adding chemicals etc. The solubility of a salt is dependent on several factors such as pH and temperature.

The SPP ionic inlet flow ($A_{i,s}^{S}$) from the feed stream and any added salt is calculated using the following equation.

$$A_{i,s}^{S} = F_{s}^{F-S} X_{i,s}^{F-S} + \sum_{m=1}^{Nm} G_{s,m}^{M} \delta_{i,s,m}^{M} \qquad s \in S, i \in I \tag{18}$$

$\delta_{i,s,m}^{M}$ represents the weight fraction of the ion in the salt being added. $\delta_{i,s,m}^{M}$ is assigned value of 0 for ions that are not part of the added salts. The ion that constitutes the produced salt and is present in the least amount dictates the maximum amount of salt that can be produced. Therefore, in order to ensure than the amount of salt produced is determined based on the limiting ion concentration, a total ion balance needs to be computed for all ions with $\delta_{i,s,n}^{N} \neq 0$, and the minimum of all ionic balances is then selected, since this would represent the actual salt amount produced based on the limiting

ion. The ionic balance is shown in Equation 20. The following equation combines the above mentioned explanation to calculate salt production rate ($G_{s,n}^{N}$).

$$G_{s,n}^{N} = \begin{cases} 0, \ \min(B_{i,s}) \leq 0 \\ \min(B_{i,s}), \ \min(B_{i,s}) > 0 \end{cases} \qquad i \in I \tag{19}$$

where $B_{i,s} = \frac{A_{i,s}^{S} - F_{s}^{S-Br} S_{n,s}^{S} MW_{i} - F_{s}^{S-Re} X_{i,s}^{S-Re} - F_{s}^{S-Lo} X_{i,s}^{S-Lo}}{\delta_{i,s,n}^{N}} \qquad s \in S, i \in I$ (20)

In the above equation, $S_{n,s}^{S} MW_{i}$ refers to the ionic outlet concentration of the brine $X_{i,s}^{S-Br}$ that is limited due to salt solubility. MW_{i} refers to the ionic molecular weight. $\delta_{i,s,n}^{N}$ represents the weight fraction of the ion in the salt being produced. $\delta_{i,s,n}^{N}$ is assigned value of 0 for ions that are not part of the produced salts. A negative value for $G_{s,n}^{N}$indicates that the amount of salt entering is less than those assigned by the exit stream concentrations. Hence in such cases, no salt production is assumed. The ionic concentration of the brine is then calculated using the following equation.

$$X_{i,s}^{S-Br} = \frac{A_{i,s}^{S} - G_{s,n}^{N} \delta_{i,s,n}^{N} - F_{s}^{S-Re} X_{i,s}^{S-Re} - F_{s}^{S-Lo} X_{i,s}^{S-Lo}}{F_{s}^{S-Br}} \qquad s \in S, i \in I \tag{21}$$

The SPP formulation is summarized in the flowchart shown below.

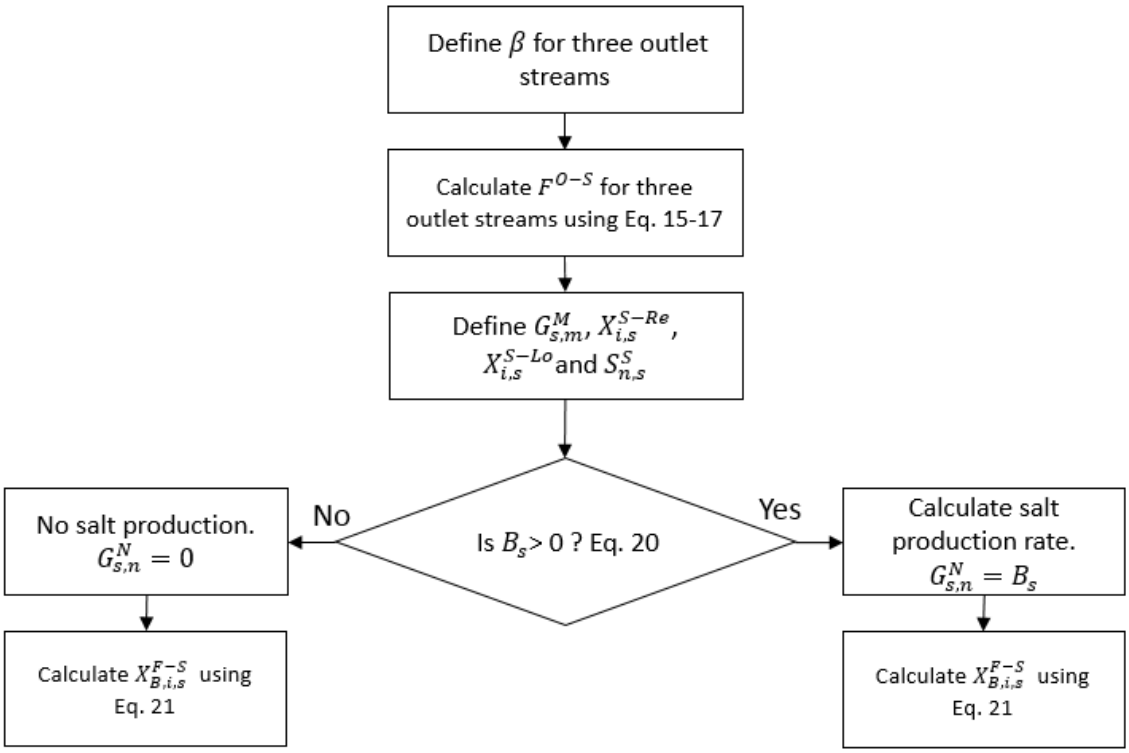

Figure 3 SPP formulation flowchart

Figure 4 summarizes the three synthesis units of the membrane and SPP superstructure.

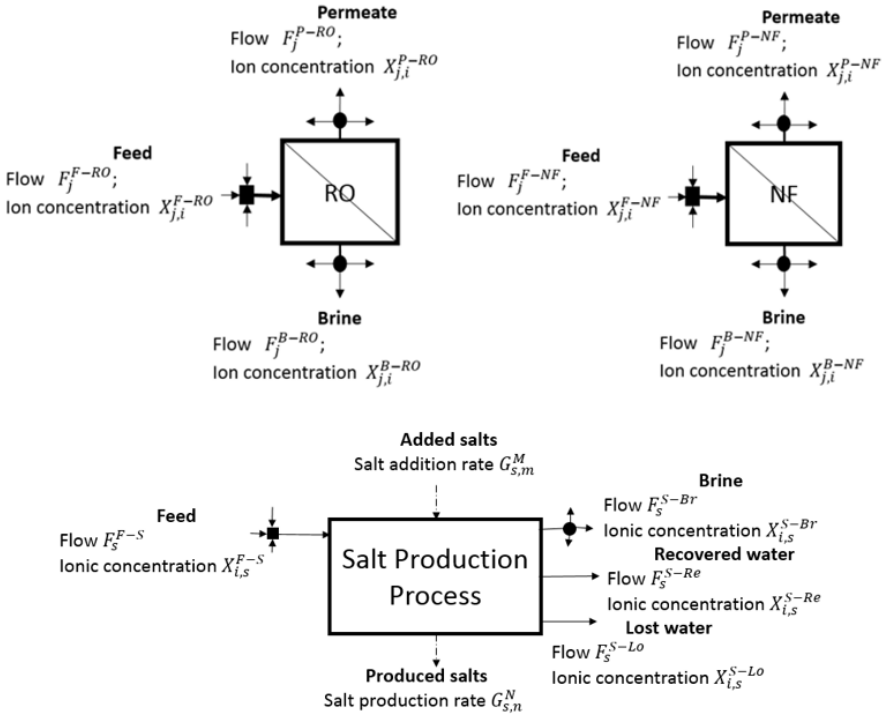

Figure 4 The three synthesis units of the superstructure: RO, NF membranes and SPP

4.4 Superstructure connectivity

A superstructure consists of all the possible connections between all the units present in the superstructure[6]. To construct a lean membrane and SPP superstructure, certain connections which are not viable are eliminated. The following sections explain the possible and eliminated connections for each type of splitter present in the superstructure.

4.4.1 Feed connectivity

The feed connectivity used in the superstructure is adopted from the work of Alnouri and Linke[18]. The seawater feed can be sent to all the membranes for desalination.

In the cases where the desalinated water concentration is lower than system limits, the seawater feed can be used to concentrate the desalinated water to meet the maximum quality limits and reduce desalination load. Thus the sweater feed can be sent to the product water mixer. The seawater feed to network brine is eliminated in order to avoid the wastage of pretreated seawater feed.

4.4.2 RO permeate connectivity

The RO membrane permeate connectivity used in the superstructure is adopted from the work of Alnouri and Linke[18]. The RO permeate can be sent to other membranes for further desalination and to the product water mixer due to its low concentration. The RO permeate is not sent to any SPP due to its low concentration of ions. The RO permeate is not sent to the network brine or recycled back into the same RO membrane since these connections would lead to the wastage of the energy spent in the desalination for that permeate stream.

4.4.3 RO brine connectivity

The RO brine can be sent to other membranes in the superstructure, to the network brine mixer and to the SPPs. At the other membranes, the RO brine can be further desalinated and at the SPPs, the high concentration of ions in the RO brine can be used to extract different salts. High salinity RO brine is not sent to the product water mixer to avoid increasing the concentration of low salinity product water. Furthermore, the recycling of RO brine back into the same membrane was eliminated to avoid increasing the concentration of the RO membrane feed which in turn increases the energy and cost requirements for that membrane.

4.4.4 NF permeate connectivity

NF permeate streams can be sent to other membranes, any SPP, the product water mixer and the network brine mixer. The NF permeate to other membrane connection is allowed for further desalination. The monovalent ion rich NF permeate stream can be sent to a SPP to extract salts comprising of such monovalent ions such as NaCl. Low quality NF permeate streams can be sent to the product water mixer. Since the overall salt rejection of NF membranes is not as high as those of RO membranes[37], NF permeate streams of higher than product water quality that are not required for further desalination or salt extraction, can be sent to the network brine mixer. Similar to RO permeate streams, NF permeate streams are also not recycled back into the same NF membrane.

4.4.5 NF brine connectivity

NF brine streams can be sent to other membranes, any SPP and the network brine mixer. The NF brine to other membrane connection is allowed for further desalination. The divalent ion rich NF brine stream can be sent to a SPP to extract salts comprising of divalent ions such as $CaSO_4$ and $MgSO_4$. NF brine streams that are not further desalinated or required for salt extraction can be sent to the network brine mixer. Since the NF brine concentration is always higher than that of the NF feed stream, it is not connected to the product water mixer. Similar to RO brine streams, NF brine streams are also not recycled back into the same NF membrane.

4.4.6 SPP connectivity

The SPP model has three outlet streams: brine, recovered water and lost water. The outlet brine streams from a SPP can be sent to other SPPs, any membrane in the superstructure and the network brine mixer. The total concentration and composition of the brine streams from SPPs depends on the individual performance of the SPP. Furthermore, the SPP outlet brine streams can consist of ions that can be extracted as salts by another SPP, allowing for the connection between one SPP to another SPP to exist. Therefore the brine streams are connected to other SPPs too. Since the recovered water is of high purity, it is only connected to the product water mixer. The lost water stream is only connected to its respective outlet mixer.

The final superstructure combines the connectivity of all the splitter types mentioned above. A lean superstructure consisting of four membranes, two RO and two NF membranes, and two SPPs is shown in Figure 5.

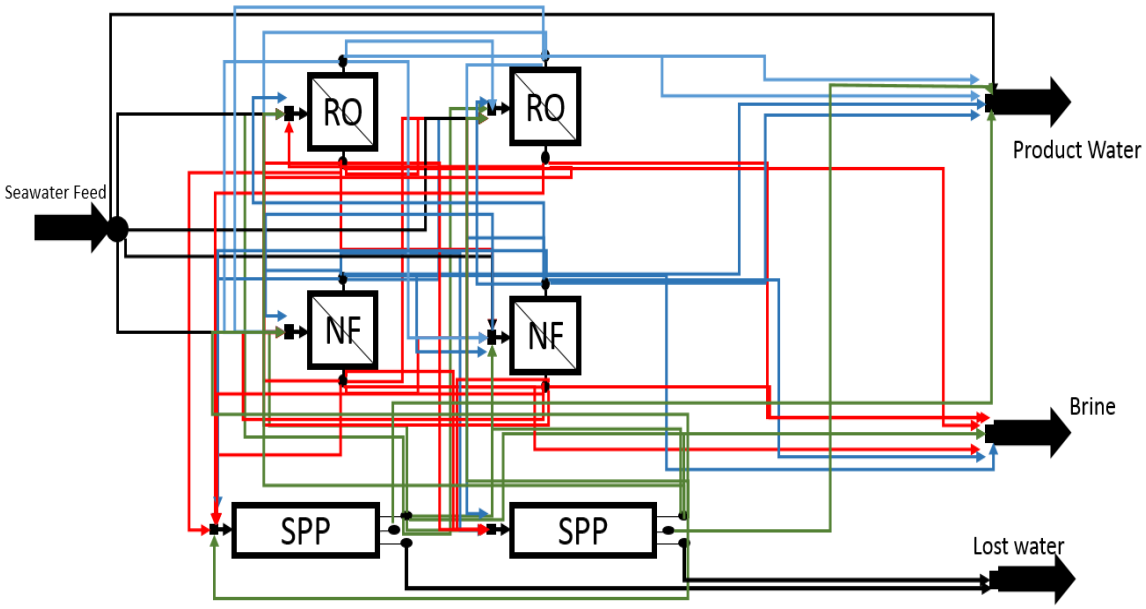

Figure 5 Superstructure consisting of 2 RO, 2 NF membranes and 2 SPPs

5. SUPERSTRUCTURE FORMULATION

The superstructure consists of four types of splitters: seawater feed, membrane permeate, membrane brine and SPP outlet streams. Flow balance equations for each of these kind of splitters ensure that the sum of the split fractions around these splitters is one. Equations 22-25 presents these splitter balance equations.

For the seawater feed splitter, the feed can be sent to a membrane *j*, whose membrane type is decided by the binaries, along with directly sending it to the final permeate mixer.

$$\sum_{j=1}^{Nm} f_j^{FEED-RO} y_j^{FEED-RO} + \sum_{j=1}^{Nm} f_j^{FEED-NF} y_j^{FEED-NF} + f^{FEED-PROD} = 1 \quad j \in J \quad (22)$$

For the permeate splitters, the stream can be sent to any other membrane *j*, product water mixer, network brine mixer and to a SPP depending on the membrane type.

$$\sum_{j\prime=1}^{Nm} f_{j,j'}^{PRO-RO} y_{j,j\prime}^{PRO-RO} + \sum_{j\prime=1}^{Nm} f_{j,j\prime}^{PRO-NF} y_{j,j\prime}^{PRO-NF} + f_j^{PRO-PROD} y_j^{PRO-PROD} +$$

$$\sum_{j\prime=1}^{Nm} f_{j,j'}^{PNF-RO} y_{j,j\prime}^{PNF-RO} + \sum_{j\prime=1}^{Nm} f_{j,j\prime}^{PNF-NF} y_{j,j\prime}^{P-NFNF} + f_j^{PNF-PROD} y_j^{PNF-PROD} +$$

$$f_j^{PNF-BRINE} y_j^{PNF-BRINE} + f_{js}^{PNF-S} y_j^{PNF-S} = 1 \qquad j, j' \in J, j \neq j', s \in S \quad (23)$$

For the brine splitters, the stream can be sent to any other membrane *j*, network brine mixer and to a SPP.

$$\sum_{j\prime=1}^{Nm} f_{j,j'}^{BRO-RO} y_{j,j\prime}^{BRO-RO} + \sum_{j\prime=1}^{Nm} f_{j,j\prime}^{BRO-NF} y_{j,j\prime}^{BRO-NF} + f_j^{BRO-BRINE} y_j^{BRO-BRINE} +$$

$$f_{js}^{BRO-S} y_j^{BRO-S} + \sum_{j\prime=1}^{Nm} f_{j,j'}^{BNF-RO} y_{j,j\prime}^{BNF-RO} + \sum_{j\prime=1}^{Nm} f_{j,j\prime}^{BNF-NF} y_{j,j\prime}^{BNF-NF} +$$

$$f_j^{BNF-BRINE} y_j^{BNF-BRINE} + f_{js}^{BNF-S} y_j^{BNF-S} = 1 \qquad j, j' \in J, j \neq j', s \in S \quad (24)$$

For the SPP outlet splitters, the stream can be sent to all the mixing nodes in the superstructure.

$$\sum_{j=1,s=1}^{Nm,Ns} f_{s,j}^{S-RO} y_{s,j}^{S-RO} + \sum_{j=1,s=1}^{Nm,Ns} f_{s,j}^{S-NF} y_{s,j}^{S-NF} + \sum_{s=1}^{Ns} f_{s,s'}^{S-S} y_{s,s'}^{S-S} + f_s^{BRINE} = 1$$

$$j \in J, s \in S, s \neq s' \tag{25}$$

The superstructure consists of five types of mixing nodes: membrane feed, network brine, product water, lost water and SPP feed. The membrane feed mixer can be for either a RO or a NF membrane depending on the membrane type. Flow and component balance equations around each of these mixers is formulated to ensure mass balance constraints are met. Equations 26 and 27 describe the flow and component balance around the feed mixer at the RO membrane *j*. The mixer can receive streams from the feed splitter, permeate and brine splitters of any membrane and any SPP brine splitter.

$$F_j^{F-RO} = F^{FEED} f_j^{FEED-RO} y_j^{FEED-RO} + \sum_{j=1}^{Nm} F_{j'}^{P-RO} f_{j',j}^{PRO-RO} y_{j',j}^{PRO-RO} +$$

$$\sum_{j=1}^{Nm} F_{j'}^{P-NF} f_{j',j}^{PNF-RO} y_{j',j}^{PNF-RO} + \sum_{j=1}^{Nm} F_{j',j}^{BRO} f_{j',j}^{BRO-RO} y_{j',j}^{BRO-RO} +$$

$$\sum_{j=1}^{Nm} F_{j'}^{B-NF} f_{j',j}^{BNF-RO} y_{j',j}^{BNF-RO} + \sum_{j=1,s=1}^{Nm,Ns} F_s^{S-Br} f_{s,j}^{S-RO} y_{s,j}^{S-RO}$$

$$j, j' \in J, j \neq j', s \in S \tag{26}$$

$$F_j^{F-RO} X_{i,j}^{F-RO} = F^{FEED} X_i^{FEED} f_j^{FEED-RO} y_j^{FEED-RO} +$$

$$\sum_{j=1}^{Nm} F_{j'}^{P-RO} X_{i,j'}^{P-RO} f_{j',j}^{PRO-RO} y_{j',j}^{PRO-RO} + \sum_{j=1}^{Nm} F_{j'}^{P-NF} X_{i,j'}^{P-NF} f_{j',j}^{PNF-RO} y_{j',j}^{PNF-RO} +$$

$$\sum_{j=1}^{Nm} F_{j'}^{B-RO} X_{i,j'}^{B-RO} f_{j',j}^{BRO-RO} y_{j',j}^{BRO-RO} + \sum_{j=1}^{Nm} F_{j'}^{B-NF} X_{i,j'}^{B-NF} f_{j',j}^{BNF-RO} y_{j',j}^{BNF-RO} +$$

$$\sum_{j=1,s=1}^{Nm,Ns} F_s^{S-Br} X_{i,s}^{S-Br} f_{s,j}^{S-RO} y_{s,j}^{S-RO} \qquad j, j' \in J, j \neq j', s \in S, i \in I \tag{27}$$

Equations 28 and 29 describe the flow and component balance around the feed mixer at the NF membrane j. The mixer can receive streams from the feed splitter, permeate and brine splitters of any membrane and any SPP brine splitter.

$$F_j^{F-NF} = F^{FEED} f_j^{FEED-NF} y_j^{FEED-NF} + \sum_{j=1}^{Nm} F_{j'}^{P-RO} f_{j',j}^{PRO-NF} y_{j',j}^{PRO-NF} + \sum_{j=1}^{Nm} F_{j'}^{P-NF} f_{j',j}^{PNF-NF} y_{j',j}^{PNF-NF} + \sum_{j=1}^{Nm} F_{j'}^{B-RO} f_{j',j}^{BRO-NF} y_{j',j}^{BRO-NF} + \sum_{j=1}^{Nm} F_{j'}^{B-NF} f_{j',j}^{BNF-NF} y_{j',j}^{BNF-NF} + \sum_{j=1,s=1}^{Nm,Ns} F_s^{S-Br} f_{s,j}^{S-NF} y_{s,j}^{S-NF}$$

$$j, j' \in J, j \neq j', s \in S \quad (28)$$

$$F_j^{F-NF} X_{i,j}^{F-NF} = F^{FEED} X_i^{FEED} f_j^{FEED-NF} y_j^{FEED-NF} + \sum_{j=1}^{Nm} F_{j'}^{P-RO} X_{i,j'}^{P-RO} f_{j',j}^{PRO-NF} y_{j',j}^{PRO-NF} + \sum_{j=1}^{Nm} F_{j'}^{P-NF} X_{i,j'}^{P-NF} f_{j',j}^{PNF-NF} y_{j',j}^{PNF-NF} + \sum_{j=1}^{Nm} F_{j'}^{B-RO} X_{i,j'}^{B-RO} f_{j',j}^{BRO-NF} y_{j',j}^{BRO-NF} + \sum_{j=1}^{Nm} F_{j'}^{B-NF} X_{i,j'}^{B-NF} f_{j',j}^{BNF-NF} y_{j',j}^{BNF-NF} + \sum_{j=1,s=1}^{Nm,Ns} F_s^{S-Br} X_{i,s}^{S-Br} f_{s,j}^{S-NF} y_{s,j}^{S-NF} \quad j, j' \in J, j \neq j', s \in S, i \in I \quad (29)$$

Equations 30 and 31 describe the flow and component balance around the product water mixer. The product water mixer can receive streams from the feed splitter, permeate stream splitter of any membrane and any SPP recovered water stream.

$$F^{PROD} = F^{FEED} f^{FEED-PROD} + \sum_{j=1}^{Nm} f_j^{PRO-PROD} F_j^{P-RO} y_j^{PRO-PROD} + \sum_{j=1}^{Nm} f_j^{P-NF} F_j^{PNF-PROD} y_j^{PNF-PROD} + \sum_{s=1}^{Ns} f_s^{S-PROD} F_s^{S-Re} \quad j \in J, , s \in S \quad (30)$$

$$F^{PROD} X_i^{PROD} = F^{FEED} X_i^{FEED} f^{FEED-PROD} + \sum_{j=1}^{Nm} f_j^{PRO-PROD} F_j^{P-RO} X_{i,j}^{P-RO} y_j^{PRO-PROD} + \sum_{j=1}^{Nm} f_j^{P-NF} F_j^{PNF-PROD} X_{i,j}^{PNF-PROD} y_j^{PNF-PROD} + \sum_{s=1}^{Ns} f_s^{S-PROD} F_s^{S-Re} X_{i,s}^{S-Re}$$

$$j \in J, s \in S, i \in I \quad (31)$$

Equations 32 and 33 describe the flow and component balance around the network brine mixer. The network brine mixer can receive streams from the permeate stream

splitter of any NF membrane, the brine splitter of any membrane and any SPP brine splitter.

$$F^{BRINE} = \sum_{j=1}^{Nm} f_j^{BRO-BRINE} F_j^{B-RO} y_j^{BRO-BRINE} + \sum_{j=1}^{Nm} f_j^{BNF-BRINE} F_j^{B-NF} y_j^{BNF-BRINE} + \sum_{j=1}^{Nm} f_j^{PNF-BRINE} F_j^{P-NF} y_j^{PNF-BRINE} + \sum_{s=1}^{Ns} f_s^{S-BRINE} F_s^{S-Br} \qquad j \in J, s \in S \tag{32}$$

$$F^{BRINE} X_i^{BRINE} = \sum_{j=1}^{Nm} f_j^{BRO-BRINE} F_j^{B-RO} X_{i,j}^{B-RO} y_j^{BRO-BRINE} + \sum_{j=1}^{Nm} f_j^{BNF-BRINE} F_j^{B-NF} X_{i,j}^{B-NF} y_j^{BNF-BRINE} + \sum_{j=1}^{Nm} f_j^{PNF-BRINE} F_j^{P-NF} X_{i,j}^{P-NF} y_j^{PNF-BRINE} + \sum_{s=1}^{Ns} f_s^{S-BRINE} F_s^{S-Br} X_{i,s}^{S-Br}$$

$$j \in J, s \in S, i \in I \tag{33}$$

Equations 34 and 35 describe the flow and component balance around any SPP feed mixer. The SPP feed mixer can receive streams from the permeate stream splitter of any NF membrane, the brine splitter of any membrane and any other SPP brine splitter.

$$F_s^{F-S} = \sum_{j=1}^{Nm} f_j^{BRO-S} F_j^{B-RO} y_j^{BRO-S} + \sum_{j=1}^{Nm} f_j^{PNF-S} F_j^{P-NF} y_j^{PNF-S} + \sum_{j=1}^{Nm} f_j^{BNF-S} F_j^{B-NF} y_j^{BNF-S} + \sum_{s=1}^{Ns} f_{s,s'}^{S-S} F_s^{S-Br} \qquad j \in J, s, s' \in S, s \neq s' \tag{34}$$

$$F_s^{F-S} X_{i,s}^{F-S} = \sum_{j=1}^{Nm} f_j^{BRO-S} F_j^{B-RO} X_{i,j}^{B-RO} y_j^{BRO-S} + \sum_{j=1}^{Nm} f_j^{PNF-S} F_j^{P-NF} X_{i,j}^{P-NF} y_j^{PNF-S} + \sum_{j=1}^{Nm} f_j^{BNF-S} F_j^{B-NF} X_{i,j}^{B-NF} y_j^{BNF-S} + \sum_{s=1}^{Ns} f_{s,s'}^{S-S} F_s^{S-Br} X_{i,s}^{S-Br}$$

$$i \in I, j \in J, s, s' \in S, s \neq s' \tag{35}$$

Equation 36-37 describe the flow and component balance around any outlet lost water mixer. The lost water mixer can receive streams only from SPP outlet streams.

$$F^{LOST} = \sum_{s=1}^{Ns} F_s^{S-Lo} \quad s \in S \tag{36}$$

$$F^{LOST} X^{LOST} = \sum_{s=1}^{Ns} F_s^{S-Lo} X_s^{S-Lo} \qquad s \in S, i \in I \tag{37}$$

Equation 38 describe the overall flow balance of the system. The seawater feed flowrate F^{FEED} must equal the sum of the flows of the product water stream F^{PROD}, network brine stream F^{BRINE} and the lost water stream F^{LOST}.

$$F^{FEED} = F^{BRINE} + F^{PROD} + F^{LOST} \tag{38}$$

Equations 39-45 set the limits on the concentration and flow of the product water stream, feed pressure of the membranes and the number of modules in each membrane.

$$X^{PROD} \leq X^{PROD,MAX} \tag{39}$$

$$X_i^{PROD} \leq X_i^{PROD,MAX} \quad i \in I \tag{40}$$

$$F^{PROD} = F^{PROD,MIN} \tag{41}$$

$$P_j^{F-RO} \leq P_j^{F-RO,MAX} \quad j \in J \tag{42}$$

$$P_j^{F-NF} \leq P_j^{F-NF,MAX} \quad j \in J \tag{43}$$

$$NM_j^{RO-MIN} \leq NM_j^{RO} \leq NM_j^{RO-MAX} \qquad j \in J \tag{44}$$

$$NM_j^{NF-MIN} \leq NM_j^{NF} \leq NM_j^{NF-MAX} \qquad j \in J \tag{45}$$

Equation 46 determines the TDS of the seawater feed stream by summing up the component concentrations in the stream. Similarly, the TDS of all the streams in the superstructure is determined by using a similar equation where the component concentrations are added to determine the TDS of the stream.

$$X^{FEED} = \sum_{i=1}^{Nc} X_i^{FEED} \quad i \in I \tag{46}$$

Equations 47-52 determine the initial and final pressure of each type of stream connection in the superstructure. The seawater feed pressure (P^{FEED}), product water pressure (P^{PROD}), network brine pressure (P^{BRINE}), feed pressure of a SPP *s* (P_s^{F-S}),

pressure of the outlet streams from the SPP, pressure drop across a RO and NF membrane (ΔP_j) need to be defined so that they can be used for the following calculations.

$$P_j^{P-RO} = P^{PROD} \qquad j \in J \tag{47}$$

$$P_j^{P-NF} = P^{PROD} \qquad j \in J \tag{48}$$

$$P_j^{B-RO} = P_j^{F-RO} - \Delta P_j^{RO} \qquad j \in J \tag{49}$$

$$P_j^{B-NF} = P_j^{F-NF} - \Delta P_j^{NF} \qquad j \in J \tag{50}$$

$$PI_j^{FEED-RO} = P^{FEED} \;\; PF_j^{FEED-RO} = P_j^{F-RO} \;\; j \in J \tag{51}$$

$$PI_{j'}^{FEED-NF} = P^{FEED} \;\; PF_{j'}^{FEED-NF} = P_j^{F-NF} \;\; j \in J \tag{52}$$

The other initial and final stream pressure specifications are provided in the Appendix section. Each stream that has a positive difference between the final and initial pressures is associated with a pump. Each stream that have a negative difference between the final and initial pressures more than a minimum specified value (ΔP^{SPEC}) is associated with an energy recovery device. The general equations for each type of connection to determine the head (H) and power required/produced (PW) by the pump/turbine were obtained from Alnouri and Linke[18] and are shown below.

$$H = \begin{Bmatrix} \frac{10.197}{SG}(PF - PI) \;\; if(\,(PF - PI)y > 0)\;\forall j' \in J \\ 0 \;\; if\big(\,(PF - PI)y = 0\big)\forall j' \in J \\ \frac{10.197}{SG}(PF - PI) \;\; if\;(PF - PI)y \;< 0 \wedge abs\Big|\, PF_{j'}^{FRO} - PI_{j'}^{FRO}\Big| > \Delta P^{SPEC}\forall j' \in J \\ 0 \;\; if\;(PF - PI)y \;< 0 \wedge abs\big|\, PF - PI\big| \;< \Delta P^{SPEC}\;\forall j' \in J \end{Bmatrix} \tag{53}$$

$$PW = \begin{cases} if\ H > 0 \ \frac{H\ F\ f\left[997.075+0.7592305\ X-0.004201(X)^{1.5}+0.00048314(X)^{2}\right]\eta^{pump}}{3.67\times10^{5}} \forall j' \in J \\ H < 0 \ \frac{H\ F\ f\left[997.075+0.7592305\ X-0.004201(X)^{1.5}+0.00048314(X)^{2}\right]}{3.67\times10^{5}\ \eta^{turb}} \forall j' \in J \end{cases} \quad (54)$$

6. CASE STUDY

The proposed approach is illustrated with a case study. The case study models a 100,000 m^3/day production capacity desalination plant with three membrane units and two SPPs. A maximum concentration limit of 500 mg/L was chosen for the product water[18]. The compositions of the two seawater feeds used in this case study are given in Table 4.

Table 4 Typical seawater composition

Formulation Notation	Ion	Concentration (mg/L)	
		Typical seawater	Eastern Mediterranean
1	Ca	400	423
2	Na	10556	11800
3	Cl	18980	21200
4	Mg	1262	1403
5	K	380	463
6	SO_4	2649	2950
7	HCO_3	140	147[38]
8	CO_3	0	0
Total dissolved solids (TDS)		34367	38396

Since a single membrane desalination train cannot produce 100,000 m^3/day of water due to membrane cleaning constraints[39], the plant was needed to be divided into several trains. This case study models the desalination facility as ten parallel trains, each producing 10,000 m^3/day of product water. The SPPs are single units and receive one combined feed from all the ten trains. The type and modelling of the membranes and the SPPs is described in the following sections.

6.1 RO membrane performance modelling

The modelling and costing of RO membranes has been adopted from the work of Alnouri and Linke[18]. They used data from Dow's membrane simulation software ROSA (Reverse Osmosis System Analysis) to develop a RO model that considers the multi ionic nature of its feed water. The operating conditions of constant 70 bar feed pressure and 25 °C temperature from their work were also assumed for this case study. Furthermore, their approach to employ post-treatment on the product water was also adopted for this work. Similar to their work, it is assumed that antiscalants that inhibit membrane fouling are used. They used an antiscalant performance prediction software, Avista Advisor Chemical Calculations Software, to determine maximum stream concentrations below which the antiscalant effectively prohibits membrane fouling. They state that for the typical seawater concentrations mentioned in Table 4, the maximum brine concentration can be 98.22 g/L. Thus this concentration limit is applied for all brine streams. The table consisting the equations adopted from their work to model RO membrane performance[18] is provided in the Appendix section.

6.2 NF membrane performance modelling

As mentioned before, there are different types of NF membranes with varied rejections of monovalent and divalent ions. For this case study, Dow's FilmTec NF270 has been chosen due to its large differences in the rejections of monovalent and divalent ions[40]. This large difference was needed since we wanted to explore how the ionic separation property of NF membranes could aid in the channeling of selective ions to

certain SPPs in the superstructure. Furthermore considerable data is available in literature regarding the performance of NF270 for desalination purposes.

A performance model for the NF270 membrane that determined the ionic rejections and permeate flux needed to be integrated into the problem formulation. Unlike RO membranes, there are large variations in the rejections, even of the same ion, of NF membranes. These rejections are a function of the feed pressure, temperature, concentration and membrane recovery[41]. Several detailed NF membrane models exist, such as Speigler-Kedeem model and Donnan steric-pore model (DSPM), that consider the several aspects of NF performance such as feed side polarization, porosity ratio, effective membrane thickness etc.[42]. Such complicated models are not applicable for incorporation in such membrane network optimization formulation. Since the objective is to approximately predict the membrane performance, a much simpler model was needed to be developed using rejection data obtained from literature or simulation software. NF270 membranes can operate up to a feed pressure of 41 bar[41]. To avoid complexity, the NF270 model was developed to be a function of only the feed concentration. Since rejections increase with increasing pressure[41] and high rejection values for divalent ions were desired, a constant high feed pressure of 30 bar was selected. Furthermore, temperature was also assumed to be constant at 25 °C during membrane operation. Membrane rejections are approximately constant at low recovery values under about 0.65 and then decrease with increasing recoveries[43 41]. Therefore, a maximum recovery constraint was enforced for all NF membranes. The NF270 membrane model as a function of only the feed concentration was developed using Dow's ROSA design software. Using the ionic

relative concentrations of typical seawater, compositions of feed streams with TDS ranging from 1000 to 40000 mg/L were calculated and used to develop the NF270 model. The maximum recovery of 0.65 was used for all simulations along with the feed pressure of 30 bar. Figure 6 presents the change in ionic rejections with feed concentration.

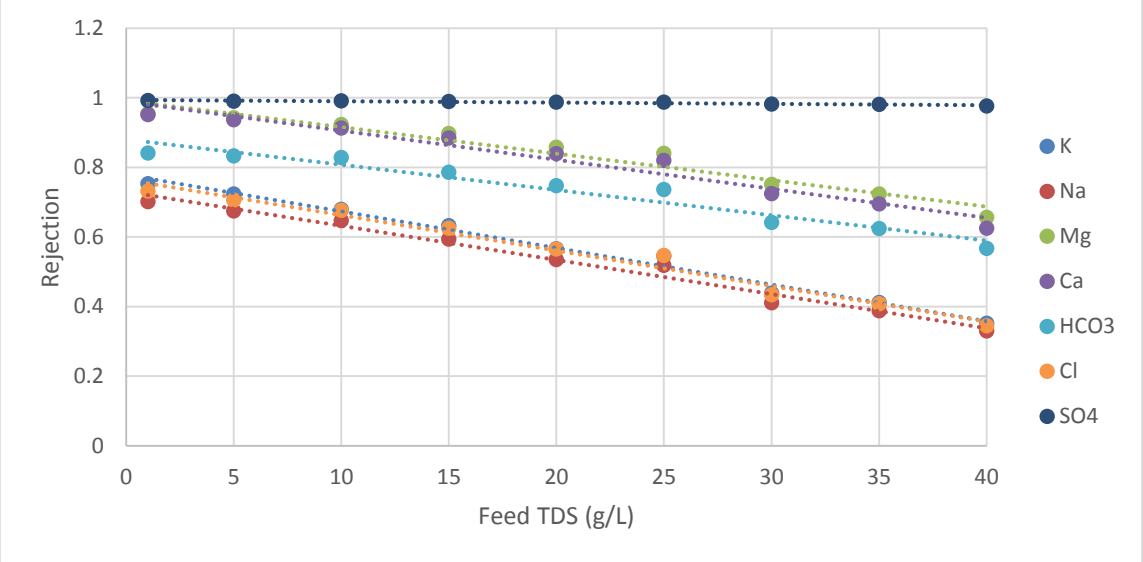

Figure 6 Change in ionic rejections with feed concentration for NF270 using ROSA

Linear regression fits were done for all the ions and the resulting fit equations which are used in the model are shown in Table 5.

Table 5 Linear fit equations for ionic rejections as a function of feed concentration

Ion	Notation	
Ca	$\gamma_{1,j}^{NF}$	$-0.0084\ X_j^{F-NF} + 0.989$
Na	$\gamma_{2,j}^{NF}$	$-0.0098\ X_j^{F-NF} + 0.7303$
Cl	$\gamma_{3,j}^{NF}$	$-0.0102\ X_j^{F-NF} + 0.7641$
Mg	$\gamma_{4,j}^{NF}$	$-0.0076\ X_j^{F-NF} + 0.9913$
K	$\gamma_{5,j}^{NF}$	$-0.0105\ X_j^{F-NF} + 0.7781$
SO_4	$\gamma_{6,j}^{NF}$	$-0.0004\ X_j^{F-NF} + 0.9938$
HCO_3	$\gamma_{7,j}^{NF}$	$-0.0073\ X_j^{F-NF} + 0.8801$

Considerable literature exists that has tested NF membrane performance for seawater feed concentrations in the range of 25 g/L to 45 g/L but little information is present on the performance on NF membranes to treat desalination brines having concentrations above 60 g/L. Since only proven processes were used and modelled in this work, a limit on the total feed concentration to every NF membrane was enforced. A maximum limit of 39 g/L, the maximum total seawater feed concentration used in this case study, was enforced. The permeate flux (Pf_j^{NF}) is calculated using the following equation from the work of Perez-Gonzalez et al.[44].

$$Pf_j^{NF} = L_s(\Delta P_m - (\pi_j^F - \pi_j^P)) \quad (55)$$

ΔP_m denotes the applied pressure, π_j^F and π_j^P the osmotic pressures of the feed and permeate streams respectively and L_s denotes the solution permeability. A conservative assumption of 0.7 10^{-6} m/s.bar was used for L_s in this work [44]. The membrane feed flow, area and permeate flux are then used to calculate the number of modules required for that NF membrane unit using Equation 55. The membrane area of an 8 unit NF270-4040 module is 298.6 m^2 [45].

$$NM_j^{NF} = \frac{F_j^{F-NF}3.6}{Pf_j^{NF}\,298.6} \tag{56}$$

Table 6 presents the membrane network parameters used in the case study.

Table 6 Case study parameters

Parameter	Value
P^{FEED} feed water pressure into the network (bar)	1
P^{PROD} final permeate pressure (bar)	1
P^{BRINE} final reject pressure (bar)	1
$F^{PROD,\ MIN}$ permeate flow required in the network (m^3/day)	100,000
$X^{PROD,\ MAX}$ maximum allowable concentration of total dissolved solids in the permeate stream (after post-treatment) (ppm)	500
$X_i^{PROD,\ MAX}$ maximum allowable concentration of dissolved Ca ions in the permeate stream (after post-treatment) (ppm)	10
$X_i^{PROD,\ MAX}$ maximum allowable concentration of dissolved Mg ions s in the permeate stream(after post-treatment) (ppm)	30
SM_j^{RO} membrane area per module for SW30HRLE-440i (6 elements/module) (m2)	245.4
SM_j^{NF} membrane area per module for NF270-440 (8 elements/module) (m2)	296.8
η^{turb} Turbine Efficiency	80%
η^{Pump} Pump Efficiency	80%
ΔP_j^{RO} pressure drop in RO unit j (bar)	1.3
ΔP_j^{NF} pressure drop in NF unit j (bar)	1
$P_j^{F,MAX}$ maximum allowable feed pressure in RO unit j (bar)	70
ΔP^{SPEC} lower end pressure difference that would allow the placement of ERDs (bar)	1
NMD_j^{MAX} maximum number of modules in one stage/pass for a constrained scenario	10000
T Temperature (C)	25
L Lifetime of plant (yr)	20
PWC Power Cost ($/kWh)	0.05
X_j Maximum brine concentration	98.22
RE_j^{NF} Maximum NF membrane recovery	0.65
X_j^{F-NF} Maximum NF membrane feed concentration	38239
$\frac{P_{NaCl}\,0.05845}{F_{21}^{O-S}}$ Maximum ratio of solid weight to solution weight in crystallizer outlet	0.4
P_{NaCl} Maximum mass of NaCl produced	200.3

6.3 Membrane network costing

The cost of the membrane network was determined using the equations developed by Alnouri and Linke[18]. A major part of the equations in their work were multiplied with a scale factor for a desalination plant of 12,000 m^3/day production capacity. Since the plant in this case study has a production capacity of 100,000 m^3/day, all the scaled equations were multiplied by a scale up factor (α_{sc}) to account for the difference in production capacity. The value of α_{sc} was determined by using the following equation

$$\alpha_{sc} = \frac{0.86\ \$/m^3}{0.51\ \$/m^3} \quad (57)$$

0.86 \$/m^3 refers to the desalination cost of producing 12,000 m^3/day of product water and 0.51 \$/m^3 refers to the desalination cost of producing 100,000 m^3/day of product water[39]. The Appendix section consists the table that presents the costing equations used to determine the capital and operating costs of the membrane network. The NF membrane cost has been obtained from the work of Mabrouk and Fath[46].

6.4 SPP 1 – $CaCO_3$ production

Softening using lime ($Ca(OH)_2$), sodium hydroxide and soda ash (Na_2CO_3) is commonly used in wastewater treatment plants. They have been suggested to be used as seawater pre-treatment steps to reduce the concentrations of the scale forming ions such as calcium and sulfate[47 48]. Furthermore, softening can also be used as brine treatment steps to extract mineral salts and reduce the concentration of the brine being disposed[32 49]. The purpose of SPP-1 is to produce calcite ($CaCO_3$) through soda ash softening. The softening is assumed to take place in a solids contact clarifier[50]. The removal of calcium ions through Na_2CO_3 softening of desalination brines has been suggested in literature[51 32]

[49]. The SPP operates at atmospheric pressure. A simplified representation of SPP-1 is shown in Figure 7.

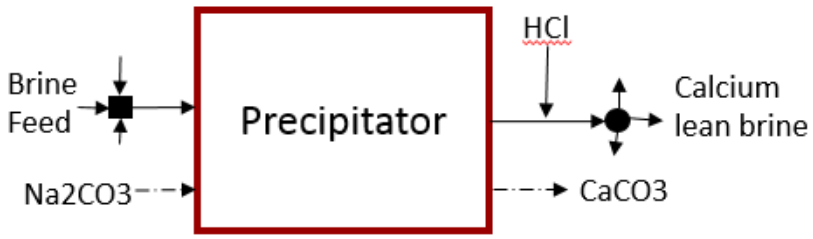

Figure 7 SPP-1 flow diagram

To study the changes in pH and verify that Na_2CO_3 softening will produce high purity calcite, the aqueous geochemical modelling software PHREEQC[52] was used. Pitzer equations were used on PHREEQC to predict the behavior of such systems. The performance of SPP-1 depends on the composition of the feed stream. Thus SPP-1 feed stream concentrations had to be modelled for PHREEQC simulations. The SPP-1 feed composition varies with changing membrane network operation. The approach used in this work to overcome this challenge was to determine the performance at both the ends of the range of the relative ionic concentrations of the SPP feed and assume that similar performance can be expected within the range. Since chloride is the most abundant ion in seawater, ionic concentrations were calculated relative to the chloride concentration. With respect to membranes, the SPP can receive streams from either a RO brine, NF permeate, NF brine splitter or any combination of the above streams. The SPP-1 feed compositions

can range from those of a NF brine from a membrane treating a NF brine (double-NF brine) to those of a NF permeate from a membrane treating a NF permeate (double-NF permeate). All other streams combinations will consist of relative ionic concentrations within this range. Thus, soda ash softening data was obtained for these two streams and the assumption was made that feed streams with relative concentrations within the range of the two streams would perform in a similar manner. The relative concentrations were calculated using the minimum rejections and a maximum recovery of 65%. Brine concentration increases with recovery and hence the maximum recovery was used. Permeate concentrations do not depend on the recovery. The maximum concentration of a stream in this system due to antiscalant restrictions is 98.22 g/L[18]. Assuming the SPP receives a stream of approximately this concentration level, the final concentrations of the two solutions were calculated and are shown in Table 7. Since a high SPP feed concentration is assumed, the minimum NF270 rejections assumption is justified. The two model solutions with their concentration data are also shown in Table 7.

Table 7 Concentrations of model double-permeate and double-brine streams

	Relative Concentrations			Final Concentrations	
	Typical Seawater	Double NF-Brine	Double NF-Permeate	Double NF-Brine	Double NF-Permeate
Ca	0.0211	0.0366	0.0069	1681.81	414.68
Mg	0.0665	0.1219	0.0182	5594.52	1099.31
Na	0.5562	0.5384	0.5805	24716.07	35012.81
K	0.0200	0.0204	0.0195	935.94	1178.00
SO_4	0.1396	0.4107	0.0002	18853.57	11.35
HCO_3	0.0074	0.0116	0.0032	531.06	193.93
Cl	1	1	1	45907.03	60309.92
			Total	98220.00	98220.00

Assuming that the membrane network has minimal effect on the pH of the streams, the typical seawater pH of 8.1 was used as the feed stream pH for the PHREEQC simulations of the two model streams. The calcium ion molar equivalent Na_2Co_3 was added in the simulations. The results of the simulations are provided in Table 8.

Table 8 PHREEQC simulation results for calcite precipitation

	Double-NF Brine	Double-NF Permeate
Calcite purity (wt %)	100	100
Fraction conversion = $\frac{CaCO3}{Na2CO3}$	0.985	0.948
Final pH	8.312	8.563

The PHREEQC results showed that 100% pure calcite can be expected with a less than 0.5 change in pH for both the streams. Furthermore, high conversions of soda ash were noticed. Thus, stoichiometric removal of calcium was assumed i.e. one mole of Na_2CO_3 leads to the production of one mole of $CaCO_3$.

Due to mixing limitations in the softening precipitator, the minimum calcium hardness that can be achieved is 30 mg/L as $CaCO_3$[53]. This minimum calcium concentration of 12 mg/L was assumed as the calcium concentration in the outlet stream. Since there was no loss of water in the clarifier, output flow was equal to the feed flow. The outlet from the precipitator has a pH slightly higher than the feed pH of 8.1 and since the membrane network was assumed to function at a constant pH of 8.1, HCl was modelled to be added to the precipitator outlet to reduce the pH to 8.1. Using PHREEQC, this HCl addition was determined to be minimal and a conservative estimate of 0.01 mol/L of HCl

addition was used. For SPP-1, Equations 15-21 are solved using the input set values and parameters shown in Table 9.

Table 9 Input model parameters for SPP-1

Sets	Value
S	1
M	2
N	1
Parameters	
$S_{1,1}^{S}$	0.3
$G_{1,1}^{M}$	$G_{1,1}^{N}$ 1.06
$G_{1,2}^{M}$	0.001 F_{1}^{F-S} 36450
$\delta_{i,1,1}^{M}$	[0, 0.434, 0, 0, 0, 0, 0, 0.566]
$\delta_{i,1,2}^{M}$	[0, 0, 0.972, 0, 0, 0, 0, 0]
$\delta_{i,1,1}^{N}$	[0.4, 0, 0, 0, 0, 0, 0, 0.6]
β_{1}^{S-Br}	1
β_{1}^{S-Re}	0
β_{1}^{S-Lo}	0

6.5 SPP 2 - NaCl production

The purpose of this SPP is to produce sodium chloride (NaCl) in two steps. Initially, a solar evaporation pond is used to evaporate water until precipitation of any salt takes place. The evaporation is stopped at this point and the pond stream is sent to a vapor recompression evaporative crystallizer. At the crystallizer, the feed is evaporated to produce salt and a concentrated slurry (exit brine). The evaporated water is condensed in the heat exchanger of the crystallizer and sent to the product water mixer due to its high purity. Such a configuration to treat desalination brines has been commonly used in ZLD schemes[54] [55]where a Multiple-effect Distillation (MED) process is used to evaporate the

water before sending it to the crystallizer. In this work, a solar pond is used to avoid the high costs of MED operation. Such use of solar ponds to concentrate brine before salt removal has been proposed in several publications[56 32 57]. The SPP operates at atmospheric pressure. A simplified SPP-2 flowsheet is shown in Figure 8.

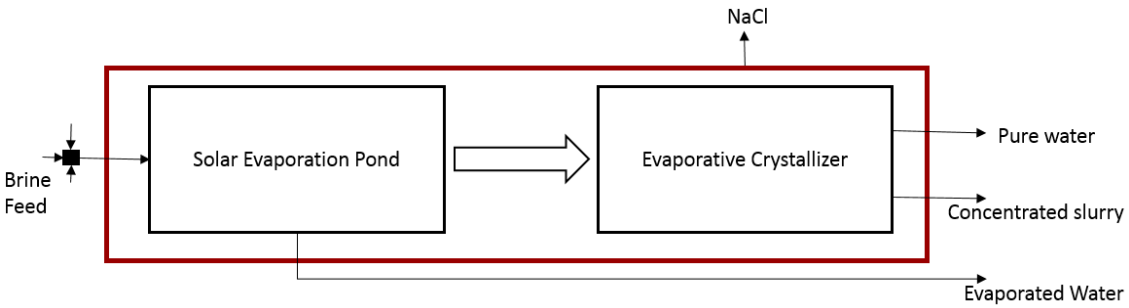

Figure 8 Simplified SPP-2 flowsheet

The solar pond is used to evaporate water until the onset of the precipitation of any salt. To model the performance of the solar pond, the solubilities of salts that precipitate the first due to supersaturation were required. The solubility of salts change in the presence of other ions. Therefore the commonly reported solubility data cannot be used in the case of studying seawater supersaturation. The crystallization of salts from concentrated aqueous solutions is a function of the pH, temperature and individual ionic concentration. The approach used in this work to obtain salt solubility values was to obtain salt solubilities for the two end of range solutions presented in Table 7 and select the conservative value. PHREEQC was used to determine which salts precipitate in for the two stream compositions. The results of the PHREEQC simulations assuming feed pH of

8.1 showed that both streams are supersaturated with two salts, $CaCO_3$ and NaCl. Thus these salts would precipitate with any loss of water in the evaporation pond and the stream would be sent to the crystallizer. There is also the possibility that the outlet stream from SPP-1 is sent to SPP-2. This stream would not be supersaturated in calcium due to its low calcium concentration. Thus, PHREEQC was again used to calculate the solubility of $CaCO_3$ and NaCl at precipitation onset for the two extreme case streams but this time the calcium concentration is reduced to 12 mg/L. The obtained precipitation onset concentrations for both the solutions are shown in Table 10. Low salt solubility leads to earlier precipitation in the pond and hence larger evaporation in the crystallizer, thus increasing overall costs of the salt production process. Therefore, the minimum values of $9.77\ 10^{-4}$ and 4.79 mol/L were chosen as conservative assumptions for $CaCO_3$ and NaCl solubilities respectively as shown in Table 10.

Table 10 $CaCO_3$ and NaCl solubilties at the onset of precipitation

	Double NF-Brine	Double NF-Permeate	Conservative value chosen
$CaCO_3$ solubility at precipitation onset (mol/L)	$9.77\ 10^{-4}$	$1.30\ 10^{-3}$	$9.77\ 10^{-4}$
NaCl solubility at precipitation onset (mol/L)	4.79	5.63	4.79

The precipitation onset solubility of $CaCO_3$ ($S_{CaCO3'}$) and of NaCl ($S_{NaCl'}$) were used to determine the fraction of the feed flow that is evaporated in the pond (d_p) through the following expression.

$$d_p = \begin{cases} 0, \ \min(1 - \frac{X_{1,2}^{F-S\prime}}{S_{CaCO3\prime}}, 1 - \frac{X_{2,2}^{F-S\prime}}{S_{NaCl\prime}}) < 0 \\ \min(1 - \frac{X_{1,2}^{F-S\prime}}{S_{CaCO3\prime}}, 1 - \frac{X_{2,2}^{F-S\prime}}{S_{NaCl\prime}}), \ \min(1 - \frac{X_{1,2}^{F-S\prime}}{S_{CaCO3\prime}}, 1 - \frac{X_{2,2}^{F-S\prime}}{S_{NaCl\prime}}) \geq 0 \end{cases} \quad (58)$$

In the above equation, $1 - \frac{X_{1,2}^{F-S\prime}}{S_{CaCO3\prime}}$ and $1 - \frac{X_{2,2}^{F-S\prime}}{S_{NaCl\prime}}$ represent the fraction of feed that needs to be evaporated before $CaCO_3$ and NaCl precipitation take place respectively. Since the pond evaporation is stopped before the precipitation of any salt, the minimum of the two fractions is selected. According to the above equation, if the solution is supersaturated before entering the SPP, the value $\min(1 - \frac{X_{1,2}^{F-S\prime}}{S_{CaCO3\prime}}, 1 - \frac{X_{2,2}^{F-S\prime}}{S_{NaCl\prime}})$ will be negative and hence no evaporation occurs in the pond and the stream is sent directly to the crystallizer

In this case study, a vapor recompression crystallizer has been assumed. The saturated feed into the crystallizer is evaporated to produce high purity NaCl, a distillate stream and an exit brine slurry. The total fraction of water that is evaporated in the SPP d_t, which is the sum of the water evaporated in the pond and the crystallizer, is assigned as a variable which is solved for by the solver. To determine the amount of NaCl precipitation, the solubility of NaCl as a function of the total water removed d_t was determined using PHREEQC. To determine this relation, change in NaCl solubility with d_t plots were determined for the two stream compositions described in Table 7. A high NaCl solubility means that less salt precipitates in the crystallizer, thus decreasing the efficiency of the SPP. Hence the higher solubility curve was chosen as a conservative assumption. A quadratic fit was performed for this NaCl solubility trend. The plots along with their quadratic fits can be seen in Figure 9.

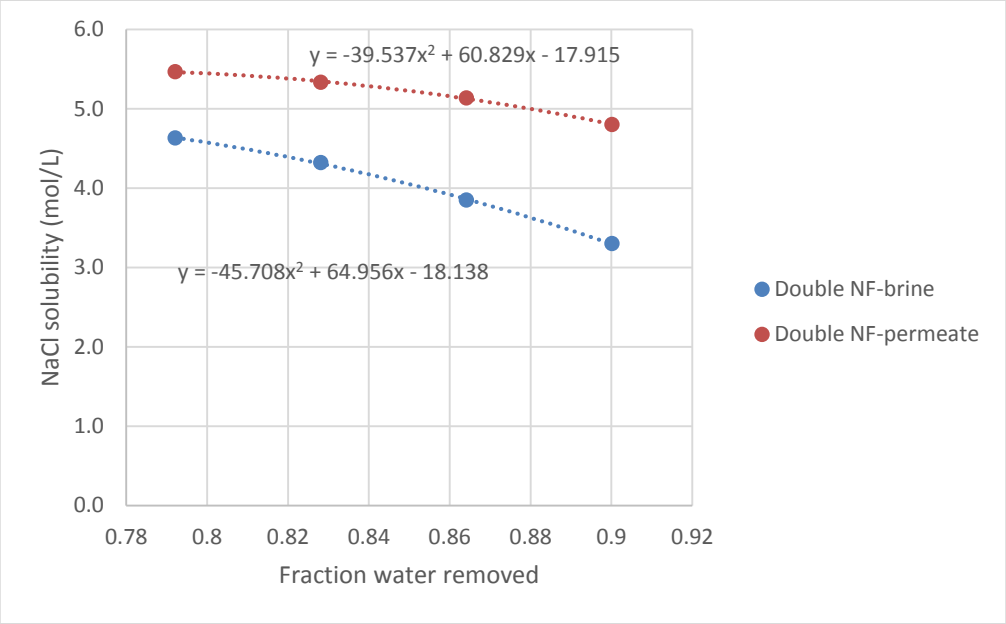

Figure 9 Exponential trends for change in NaCl solubility with total water evaporated

The concentration of the distillate stream is assumed to be 20 mg/L of NaCl[58]. Furthermore, it was assumed that no ions are lost in the evaporated water from the pond. Due to the high salinity of the exit brine from the crystallizer, this stream is only connected to the network brine mixer. For SPP-2, Equations 15-21 are solved using the input set values and parameters shown in Table 11.

Table 11 Input model parameters for SPP-2

Sets	Value
S	2
M	0
N	1
Parameters	
$S_{1,2}^{S}$	$(-21.3115\ d_t^2 + 24.7568\ d_t - 1.909)1000$
$\delta_{i,2,1}^{N}$	[0, 0.393, 0.607, 0, 0, 0, 0, 0]
$X_{i,2}^{S-Re}$	[0, 7.87, 12.13, 0, 0, 0, 0, 0]
$X_{i,2}^{S-Lo}$	[0, 0, 0, 0, 0, 0, 0, 0]
β_2^{S-Br}	$1 - d_t$
β_2^{S-Re}	$d_t - d_p$
β_2^{S-Lo}	d_p

A constraint was placed on the precipitated salts concentration in the exit brine that is sent for solids removal. A maximum ratio of solid weight to solution weight was assumed to be 0.4 [57]. A constraint was required to be placed on the production capacity of NaCl since region specific limits on the market availability for salts always exist. Qatar imports $24 million of NaCl every year[59]. Assuming a price of $65 per ton of NaCl[60], a production capacity of 1101.6 ton per day constraint was enforced. No such limit was placed on the production of $CaCO_3$ since, compared to NaCl, the production of $CaCO_3$ is negligible and has minimal influence on the plant cost analysis.

The cost equations for SPP-1 and SPP-2 are shown in Table 12. The numbers in brackets in Table 12 represent conversion in units. The values of the cost parameters (α) are given in Table 13. The capital cost of SPP-1 is the cost of the solid contact clarifier. The operating costs for SPP-1 are the cost of purchasing soda ash and selling the produced calcite. The capital cost of SPP-2 is the sum of the land cost of the evaporation pond and

capital cost of the crystallizer. The operating costs for SPP-1 are the electrical cost of the crystallizer and selling the produced NaCl.

Additional processes such as solid-liquid separation and solids drying are required to produce dry salt. Units such as centrifugal filters and rotary dryers can be used for such purposes[54]. Work that perform economic analyses of such salt production processes involving brine concentration and crystallizers do not address the costs for solid-liquid separation and solids drying[54 51 56]. Thus, for this case study it was assumed that these processes do not significantly affect the overall cost of the SPP. Hence, their capital and operating costs were not considered.

A Lang factor of 5 is used to determine the total capital investment for the equipment used [61]. The fixed operating cost of maintenance and operation is assumed to be 20 percent of the operating cost of the crystallizer [61]. Equations calculating the overall capital and operating costs for salt production are shown in Table 12.

Table 12 Cost equations for salt production processes

Capital cost of clarifier in SPP-1	$CC_{SPP-1} = \alpha_{cr}\, F_1^{F-S}\ (86.4)$
Cost of soda ash	$OC_{Na2CO3} = G_{1,1}^{M}(0.031536)\ \alpha_{Na2CO3}$
Cost of HCl	$OC_{HCl} = G_{1,2}^{M}(0.031536)\ \alpha_{HCl}$
Revenue from calcite sale	$OC_{CaCO3} = -\ G_{1,1}^{N}(0.031536)\ \alpha_{CaCO3}$
Total operating costs for SPP-1	$OC_{SPP-1} = OC_{Na2CO3} + OC_{CaCO3} + OC_{HCl}$
Capital cost of evaporation pond	$CC_{pond} = \dfrac{\alpha_p\, F_2^{F-S}\, d_p(3600)}{\alpha_{er}}$
Capital cost of crystallizer	$CC_{crys} = \alpha_C\, F_2^{F-S}\ (3.6)$
Operating cost of crystallizer	$OC_{crys} = \alpha_k\, \alpha_o\, F_2^{F-S}(1-d_p)(31536)$
Revenue from NaCl sale	$OC_{NaCl} = -G_{2,1}^{N}(0.031536)\ \alpha_{NaCl}$
Total operating costs for SPP-2	$OC_{SPP-2} = OC_{crys} + OC_{NaCl}$
Total capital investment for salt production	$TCI_{SPP} = \dfrac{(CC_{crys} + CC_{SPP-1})5 + CC_{pond}}{L}$
Total operating cost for salt production	$TOC_{SPP} = OC_{SPP-2} + OC_{SPP-1} + 0.2\ OC_{crys}$

Table 13 Case study cost parameters

Cost parameter	Value	Source
α_{cr}	36 \$/m^3/day feed	[51]
α_{CaCO3}	62 \$/ton	[62]
α_{Na2CO3}	331 \$/ton	[63]
α_{er}	417 g/m^2 h	[64]
α_p	50 \$/m^2	[65]
α_C	33000 \$/m^3/h feed	[66]
α_k	0.05 \$/kwh	[18]
α_o	0.339 kwh/m^3 feed	[54]
α_{NaCl}	65 \$/ton	[60]
α_{HCl}	85 \$/ton	[20]

6.6 Superstructure

The 3 membrane superstructure along with the 2 SPPs is shown in Figure 10.

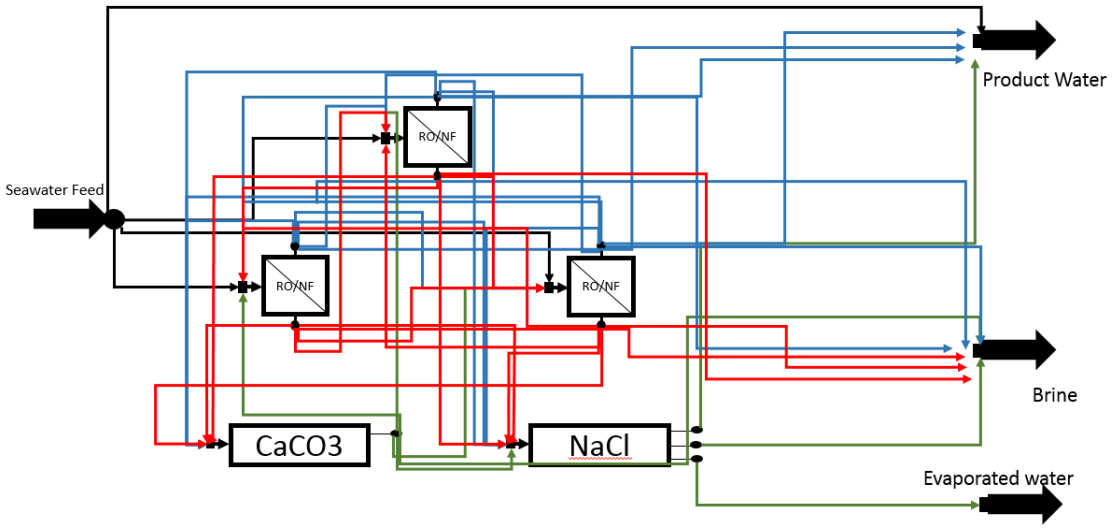

Figure 10 Case study superstructure

The case study formulation was implemented on a MS Excel 2013 interface by the global solver What'sBest! 9.0 by LINDO systems. The laptop used had an Intel Core i7-4500U processor with 1.80 GHz, 8 GB Ram and 64-bit operating system.

7. OPTIMIZATION RESULTS

For both the seawater feeds, the optimal design for the base case consisting of no salt production consists of two membranes, one RO and one NF. The entire feed is sent to the RO membrane, from which the brine is sent to the network brine mixer. A major fraction of the RO permeate is sent to the product water mixer. A portion of the RO permeate is sent for further desalination to the NF membrane. The permeate from the NF membrane is sent to the product water mixer and the NF brine is recycled back to the RO membrane. These single train least cost designs for both the seawater feeds with stream flow, concentrations, pump or turbine powers and number of membrane elements are shown in Figure 11 and 12. The large difference between the number of RO modules and the number of NF modules indicates that the major part of the desalination takes place in the RO membrane. The overall cost of the optimal design were 0.58 $/m^3 of produced water for typical seawater and 0.62 $/m^3 for eastern Mediterranean.

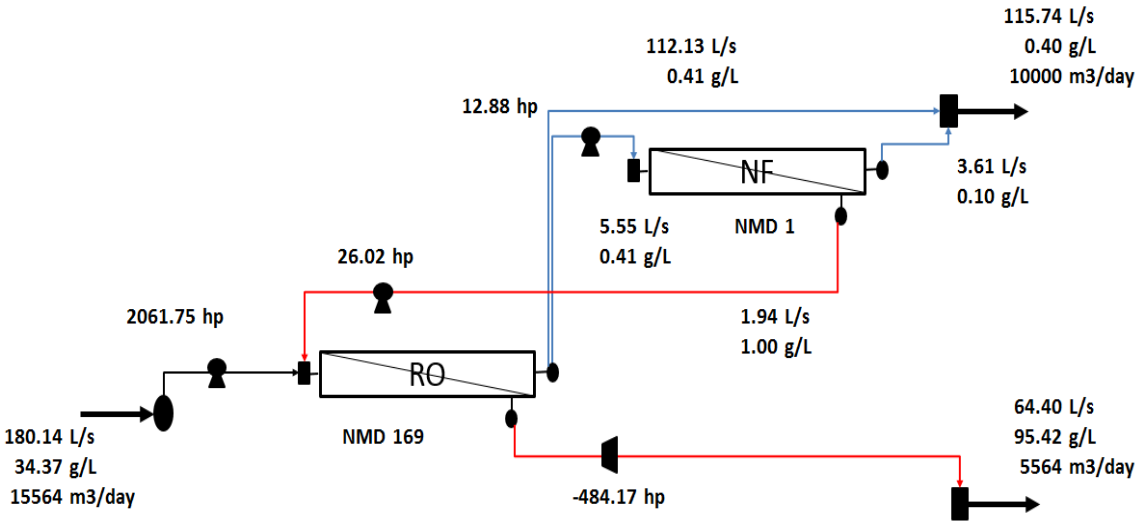

Figure 11 Optimized design of base case for typical seawater

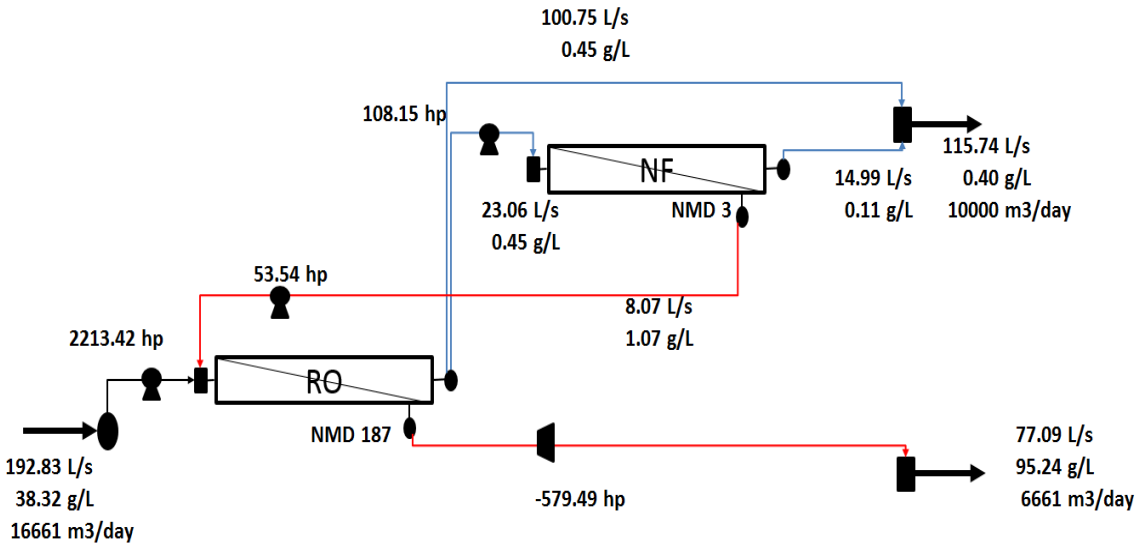

Figure 12 Optimized design of base case for eastern Mediterranean

The optimal design of the hybrid membrane and salt production network for a single train is shown in Figure 13 and 14. These figures also show the stream flows,

concentrations, pump or turbine powers and number of membrane elements. Both the least cost designs consist of two RO membranes and one NF membrane. There are two variations in the stream connections between the two seawater feeds. For the typical seawater feed, the feed is sent to the NF membrane. The NF permeate, which is rich in Na and Cl, is sent to a RO membrane. The permeate from this RO membrane is sent to the product water mixer. The brine from this RO membrane is sent to SPP-1. Thus, this RO membrane concentrates the monovalent rich NF permeate stream. The divalent rich NF brine stream is sent to another RO membrane for desalination. The permeate from this membrane is sent to the product water mixer while the brine is divided into two fractions. A small fraction of the RO brine is recycled back to the NF membrane while the other major fraction is sent to the network brine mixer. The calcium deficient outlet stream from SPP-1 is sent to the feed mixer of SPP-2. Thus, SPP-1 and SPP-2 operate in series. Since evaporation of water is cheaper in the solar pond than in the crystallizer, SPP-1 reduces the calcium concentration of the feed into SPP-2 and increases the fraction of the water that can be evaporated in the evaporation pond. The maximum amount of NaCl was produced in the crystallizer of SPP-2. The outlet streams from SPP-2 are sent to their respective mixers. For the eastern Mediterranean seawater, a minor fraction of the feed is sent to the RO membrane that receives the NF brine. The other major fraction of the feed is sent to the NF membrane. Furthermore, a fraction of the brine from this RO membrane is not recycled back to the NF membrane as in the previous case but sent to the network brine mixer in its entirety. All the other stream connections are similar to the optimal design described for the typical seawater feed case.

The compositions of a few key streams in the optimal design for both the seawater cases are provided in Table 14. The overall cost of the optimal design was 0.45 $/m^3 for the typical seawater feed and 0.46 $/m^3 for the eastern Mediterranean feed. The cost breakdown into the capital and operating costs for desalination and salt production for these designs is provided in Table 15. Table 15 also presents the cost breakdowns into the capital and operating costs for both the designs shown in Figures 11 and 12.

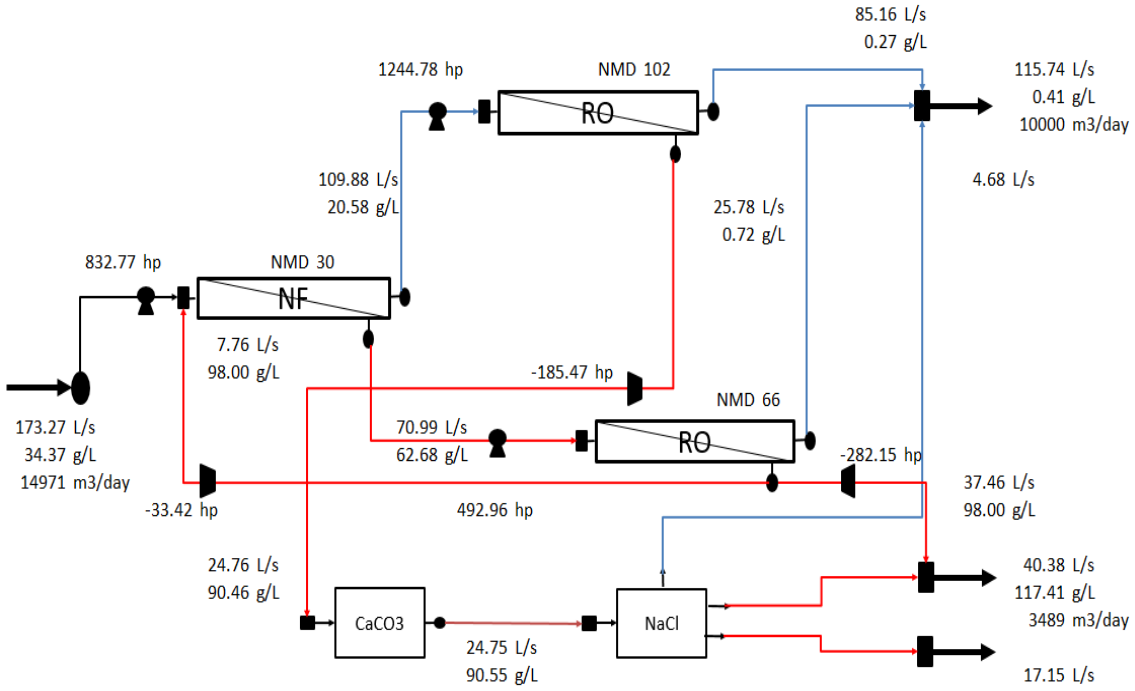

Figure 13 Optimized design with salt production for typical seawater

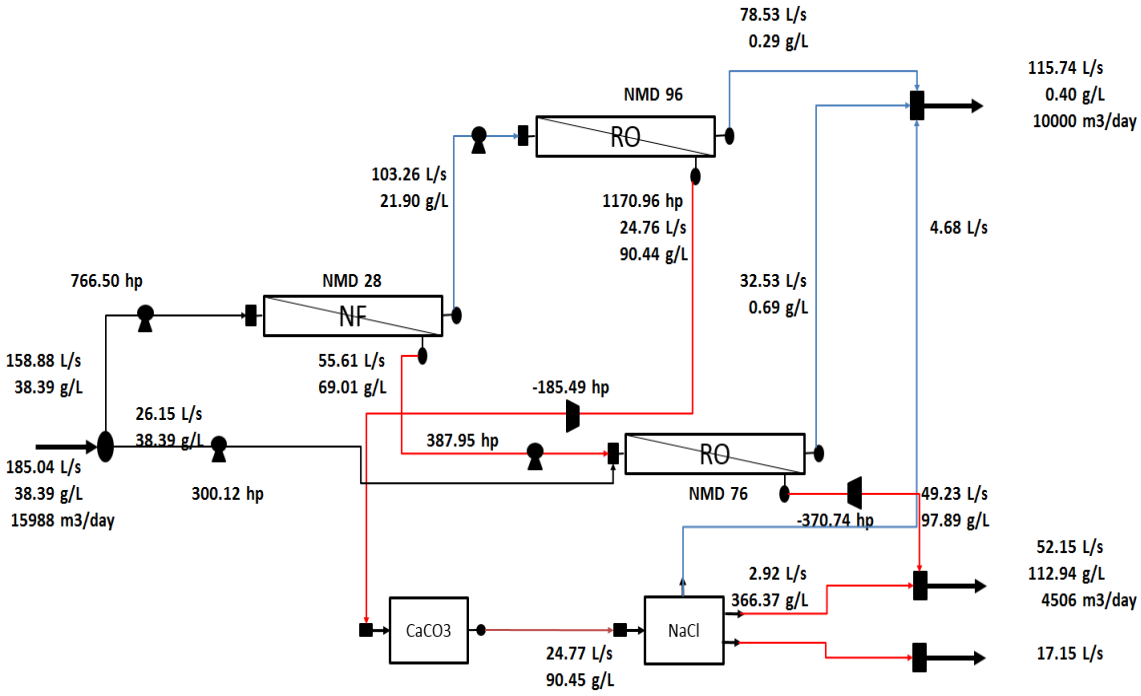

Figure 14 Optimized design with salt production for eastern Mediterranean

As shown in Table 15, the determination of optimal membrane and SPP network designs leads to the reduction of the overall plant costs. If one assumes that the desalination plant sells the product water cost at the price of producing it, then the reduction in overall costs offers the plant to sell its product water at a lower price i.e. offering a discount on the product water. This product water discount was determined by calculating the percent reduction in the total annualized costs. The water discount was determined to be 21.98% for typical sewater feed and 25.62% for eastern Mediterranean feed as mentioned in Table 15.

Table 14 Summary of key stream compositions in optimized design

Typical Seawater					
Ions	SPP-1 Feed (mg/L)	SPP-2 Feed (mg/L)	Network permeate (mg/L)	Post treatment permeate (mg/L)	Brine (mg/L)
K	1090.33	1090.33	6.50	6.50	1610.47
Na	31424.74	32141.22	137.38	137.38	33938.78
Mg	1812.82	1812.82	4.00	10.00	5403.56
Ca	635.02	12.00	1.28	30.00	1330.65
CO_3	0.00	0.00	0.00	57.82	0.00
HCO_3	262.87	262.87	2.53	2.53	593.46
SO_4	288.65	288.65	7.70	7.70	11344.31
Cl	54945.65	54945.65	248.06	248.06	63191.54
TDS	90460.10	90553.55	407.45	500.00	117412.77
Eastern Mediterranean					
Ions	SPP-1 Feed (mg/L)	SPP-2 Feed (mg/L)	Network permeate (mg/L)	Post treatment permeate (mg/L)	Brine (mg/L)
K	1190.20	1190.20	7.22	7.22	1625.78
Na	31475.02	32136.36	136.88	136.88	33052.73
Mg	1755.22	1755.22	2.91	10.00	4971.93
Ca	587.08	12.00	0.89	30.00	1225.89
CO_3	0.00	0.00	0.00	61.10	0.00
HCO_3	241.78	241.78	2.43	2.43	517.01
SO_4	265.89	265.89	5.39	5.39	10455.76
Cl	54924.76	54960.21	246.98	246.98	61088.14
TDS	90439.94	90561.66	402.70	500.00	112937.26

Table 15 Cost breakdown of base case and optimized designs along with product water discount due to optimization approach

Typical Seawater			
	Only Desalination	Desalination with SPP	% Water Discount
Membranes	RO-NF	RO-RO-NF	21.98
Total Cost ($/m^3)	0.58	0.45	
Desal. Operating ($/m^3)	0.45	0.51	
Desal. Capital ($/m^3)	0.12	0.12	
SPP Operating ($/m^3)	-	0.14	
SPP Capital ($/m^3)	-	0.24	
Salt revenue ($/m^3)	-	0.56	
Eastern Mediterranean			
	Only Desalination	Desalination with SPP	% Water Discount
Membranes	RO-NF	RO-RO-NF	25.62
Total Cost ($/m^3)	0.62	0.46	
Desal. Operating ($/m^3)	0.50	0.52	
Desal. Capital ($/m^3)	0.13	0.13	
SPP Operating ($/m^3)	-	0.14	
SPP Capital ($/m^3)	-	0.24	
Salt revenue ($/m^3)	-	0.57	

The advantage of using the proposed approach of optimizing hybrid membrane and SPP superstructure over the common approach of treating the desalination brine in an end-of-pipe (EOP) treatment for salt recovery was studied. To obtain cost results for the EOP approach, the RO-NF base case design shown in Figures 10 and 11 were optimized with SPPs. The total annualized costs for salt production with an EOP approach were 0.47 $/m^3 for typical seawater and 0.51 $/m^3 for eastern Mediterranean feed. The cost breakdown in capital and operating costs is given in Table 16. Table 16 also provides the percent differences between the total cost of the EOP treatment and the cost from the superstructure optimization. Thus, using our approach leads to 4.56% and 8.55% decrease

in the total annualized costs for the two seawater feeds considered. Other percent changes are also presented in Table 16. The membrane network costs increase in the optimized case due to the presence of an extra membrane but salt production costs decrease due to better quality streams entering the SPPs. In the EOP treatment case, the brine entering SPP-1 has a higher concentration of calcium and thus a larger amount of softening takes place, making the process more expensive than the one developed using our approach.

Table 16 Cost breakdown and comparison between typical brine treatment and hybrid membrane optimization approaches

Typical Seawater			
	EOP Salt production	Optimized salt production	% Difference
Membranes	RO-NF	RO-RO-NF	
Total Cost ($/m^3)	0.47	0.45	4.56
Desal. Operating ($/m^3)	0.43	0.51	-17.02
Desal. Capital ($/m^3)	0.12	0.12	-4.99
SPP Operating ($/m^3)	0.15	0.14	4.55
SPP Capital ($/m^3)	0.25	0.24	4.55
Salt revenue ($/m^3)	0.48	0.56	17.26
Eastern Mediterranean			
	EOP Salt production	Optimized salt production	% Difference
Membranes	RO-NF	RO-RO-NF	
Total Cost ($/m^3)	0.51	0.46	8.55
Desal. Operating ($/m^3)	0.47	0.52	-10.35
Desal. Capital ($/m^3)	0.12	0.13	-5.42
SPP Operating ($/m^3)	0.15	0.14	4.59
SPP Capital ($/m^3)	0.25	0.24	4.59
Salt revenue ($/m^3)	0.49	0.57	16.44

The major salt product in this case study is NaCl. Market prices for salts vary and depend upon several factors such as the region, salt quality etc. Prices for NaCl range from 30 $/ton to 100 $/ton[60]. For all the results presented above, the average price of 65 $/ton was chosen. The overall cost of the system depends strongly on the price of NaCl. Therefore, the superstructure formulation was solved for five prices of NaCl within the mentioned range. The five prices were chosen to be 30, 47.5, 65, 82.5 and 100 $/ton.

Table 17 provides the optimal total annualized cost of the plant for the five NaCl prices and two seawater feeds. For both the seawater feeds, when the price of NaCl is 30 $/ton and 47.5 $/ton, the base case optimal design and cost are reported. Thus at a 30 $/ton and 47.5 $/ton price of NaCl, it is economical to not produce any salt since the plant makes a loss instead of a profit by producing salt. For the other higher NaCl prices, the total annualized costs are lower than the base cases and hence the plant can afford to provide a discount on its product water price. All the optimal designs for the higher salt prices have the same membrane and SPP design as shown in Figures 11 and 12. Figure 15 plots the data given in Table 17 to display the trend in the change of total plant costs with changing NaCl prices. For the NaCl prices higher than 47.5 $/ton, the total plant costs decrease linearly with salt prices.

Table 17 Optimal total costs for different salt prices

Typical Seawater		Eastern Mediterranean	
NaCl price ($/ton)	Total Annualized Cost ($/m3)	NaCl price ($/ton)	Total Annualized Cost ($/m3)
30	0.58	30	0.62
47.5	0.58	47.5	0.62
65	0.45	65	0.46
82.5	0.27	82.5	0.29
100	0.09	100	0.11

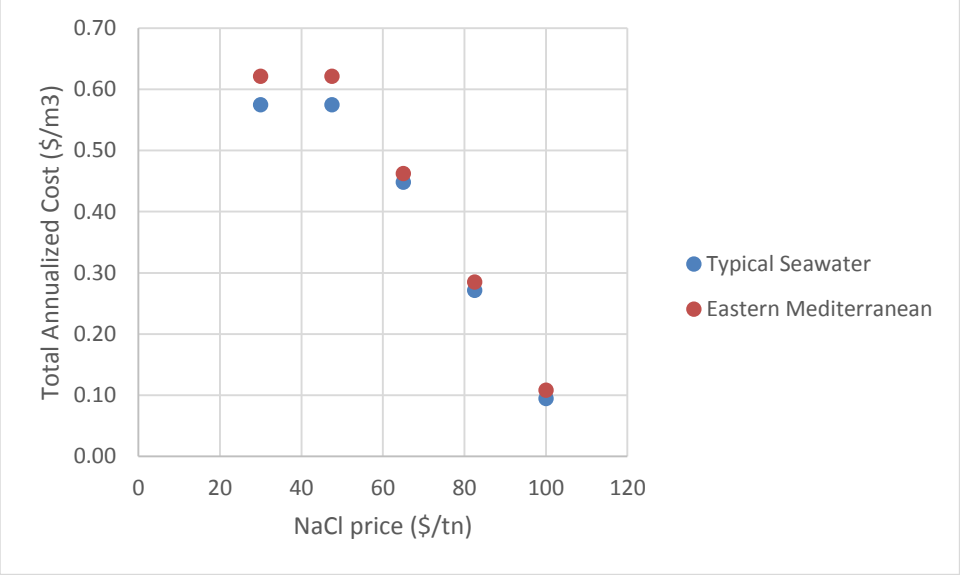

Figure 15 Change in total costs of optimal designs with increasing NaCl prices

8. APPROXIMATE LITERATURE-BASED NF MODELLING

In this work, NF270 rejections for different ions were obtained using ROSA. According to the work by Pontir et al., ROSA predictions are not accurate for NF membranes at high pressures (>10 bar) and high feed concentrations (>35 g/L). Ionic rejection data for NF270 at 30 bar for a seawater feed stream (~29 g/L feed) was obtained [40] and compared with the rejection values from ROSA at the same conditions of feed pressure, concentration and rejection. From Figure 16, it can be seen that for monovalent ions, the ROSA rejections are higher than those from literature and for divalent ions, the ROSA rejections are lower than those from literature. Thus, NF membranes using the rejection trends developed using ROSA are less effective in separating the monovalent ions from the divalent ions. Due to this poor separation by ROSA rejections, the stream sent to the SPPs is rich in calcium and hence, leads to an increase in the overall cost of the salt production processes. Therefore, it can be concluded that the optimal designs generated using ROSA rejections are conservative. Optimizing superstructures with better NF membrane models that predict rejection values closer to the ones obtained from literature will lead to the generation of less expensive designs than the ones shown before. Rejections obtained from ROSA were used in this work due to two major reasons. Firstly, as shown above, ROSA rejections can be considered to be conservative. Even through the usage of such conservative rejection values, network designs could be generated that displayed a synergy between the hybrid membranes and SPPs, eventually leading to less-expensive processes when compared to the base case and EOP salt production case.

Secondly, the ROSA rejections were used so that a simple trend representing the change in rejections with feed concentration could be developed and used in the modelling. There is a lack of such models to predict NF membrane performance that can be integrated within such optimization formulations. Furthermore, there is also a lack of rejection data in literature for NF270 membranes at high pressures and high feed concentrations that can be used to develop trends for membrane performance prediction.

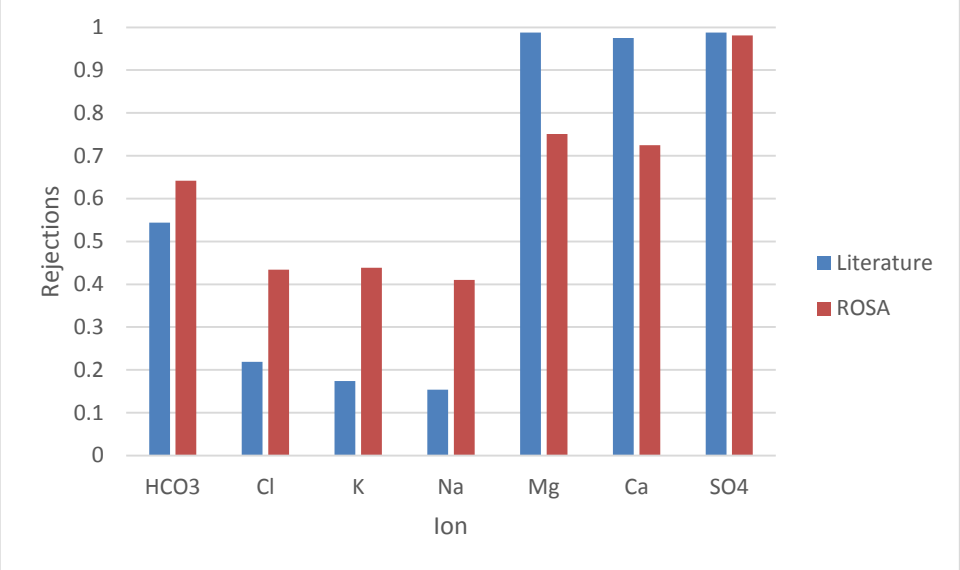

Figure 16 Comparison of rejection values from ROSA and literature

To study the effect of using more accurate NF rejections on the optimization results, rejection trends were obtained [44] and used to model NF270 performance. Rejection data was provided only for three ions: SO_4, Cl and Na. SO_4 rejection data was used for all divalent ions, Na rejections were used for all monovalent cations and Cl rejections were

used for all monovalent anions. Furthermore, a recovery of 65% was assumed for all calculations. Due to the above mentioned simplifications, the NF model developed can be described as a crude approximation. The rejection data obtained from literature is shown in Table 18. Figure 17 plots the data from Table 18 and displays the polynomial fits for these trends. The polynomial fit equations are shown in Table 19.

Table 18 Approximate NF rejection data from literature

Feed concentration (g/L)	Na	Cl	SO_4
16.2	0.35	0.07	0.89
32.5	0.15	0.04	0.85
57.7	0.09	0.04	0.70
74.0	0.06	0.04	0.61

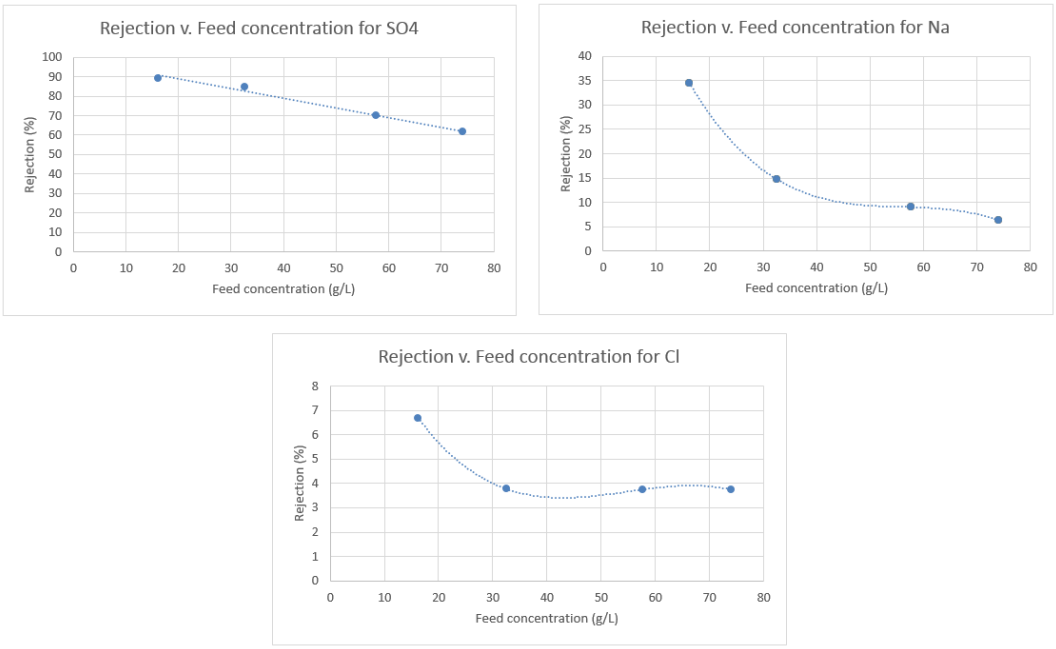

Figure 17 Rejection v. feed concentration plots for Na, Cl and SO_4 using approximate literature data

Table 19 Fit equations for ionic rejections using approximate literature data

Ion	Notation	Fit equations
Na, K	$\gamma_{2,j}^{NF}$, $\gamma_{5,j}^{NF}$	$-0.0004(X_j^{F-NF})^3 + 0.0643(X_j^{F-NF})^2 - 3.6349\, X_j^{F-NF} + 78.105$
Cl, HCO_3	$\gamma_{3,j}^{NF}$, $\gamma_{7,j}^{NF}$	$-0.00007(X_j^{F-NF})^3 + 0.0121(X_j^{F-NF})^2 - 0.6323\, X_j^{F-NF} + 14.072$
SO_4, Ca, Mg	$\gamma_{4,j}^{NF}$, $\gamma_{1,j}^{NF}$, $\gamma_{6,j}^{NF}$	$-0.4963\, X_j^{F-NF} + 98.748$

The case study superstructure was solved with the new NF model to investigate the effects it would have on the optimal designs and costs.

The optimal designs obtained for both the seawater feeds are shown in Figures 18 and 19. The same optimal design was obtained for both the seawater feeds. Table 20 presents the compositions of key streams in the optimal design. A comparison of the stream data from Table 14 with those from Table 20 shows that using more accurate NF models led to a reduction in the calcium concentration in the feed stream to SPP-1, which reduced softening costs. Furthermore, an increase in the concentrations of sodium and chloride into SPP-1 was also obtained. This increased the efficiency of SPP-2 since the major product of this SPP is NaCl.

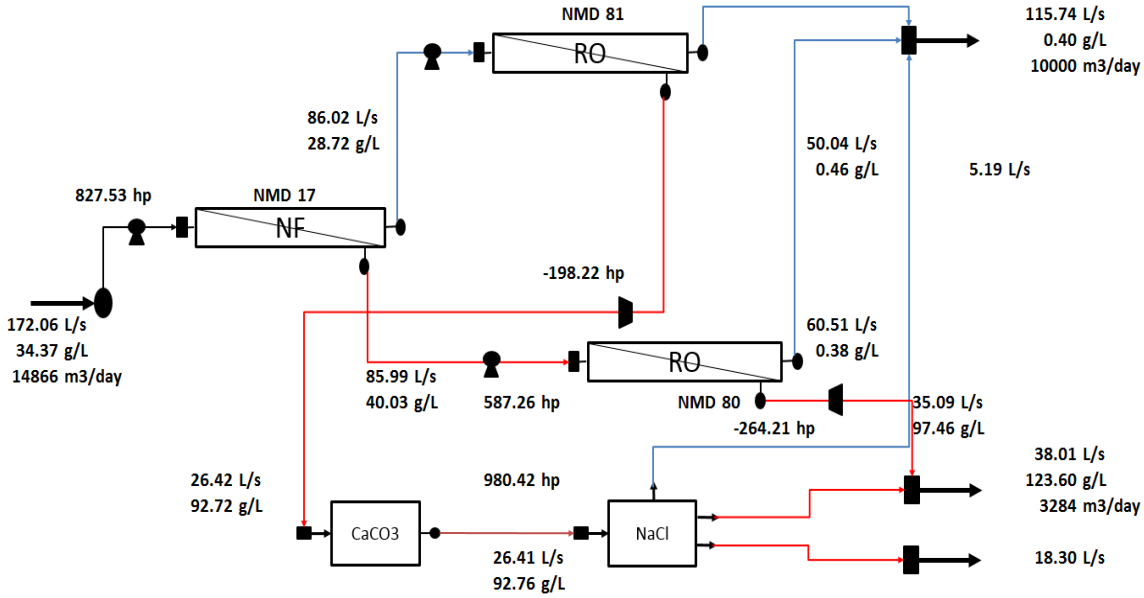

Figure 18 Optimized design with salt production for typical seawater using approximate NF model from literature

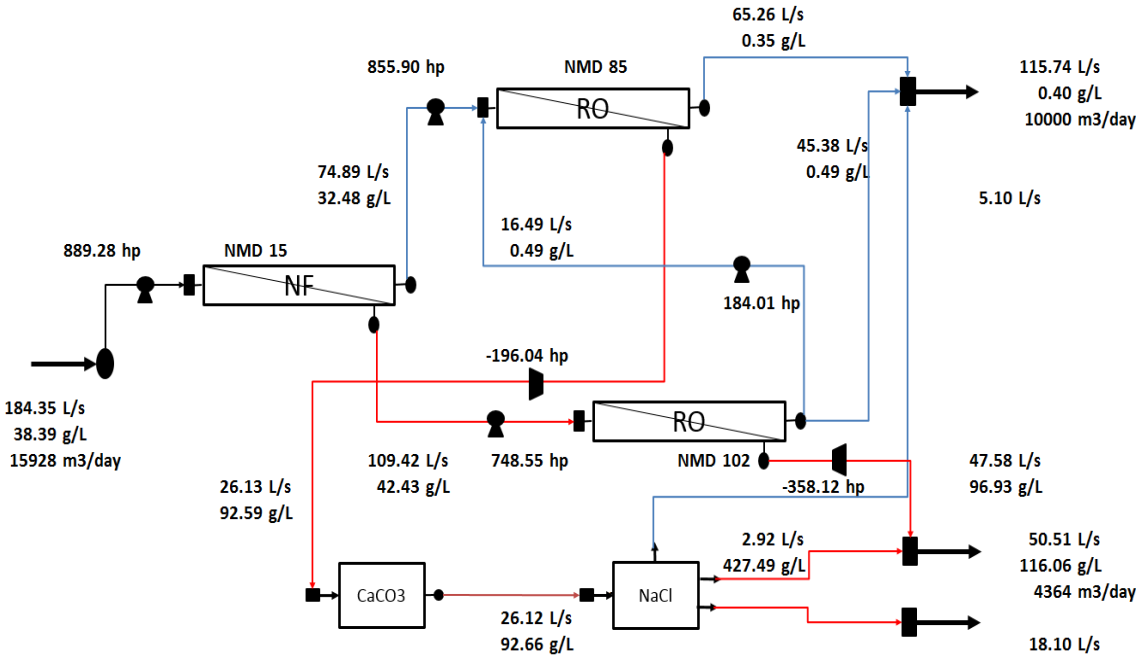

Figure 19 Optimized design with salt production for eastern Mediterranean using approximate NF model from literature

Table 20 Summary of key stream compositions in optimized design using approximate NF model from literature

Typical Seawater					
Ions	SPP-1 Feed (mg/L)	SPP-2 Feed (mg/L)	Network permeate (mg/L)	Post treatment permeate (mg/L)	Brine (mg/L)
K	1064.91	1064.91	6.60	6.60	1698.13
Na	29688.50	29949.03	135.36	135.36	35435.68
Mg	752.88	752.88	3.00	10.00	5702.69
Ca	238.54	12.00	0.95	30.00	1650.06
CO_3	0.00	0.00	0.00	60.77	0.00
HCO_3	432.39	432.39	2.84	2.84	625.00
SO_4	1580.33	1580.33	6.30	6.30	11970.23
Cl	58966.49	58966.49	248.13	248.13	66520.05
TDS	92724.04	92758.03	403.18	500.00	123601.86
Eastern Mediterranean					
Ions	SPP-1 Feed (mg/L)	SPP-2 Feed (mg/L)	Network permeate (mg/L)	Post treatment permeate (mg/L)	Brine (mg/L)
K	1175.84	1175.84	7.16	7.16	1672.33
Na	30039.24	30309.70	134.52	134.52	33786.88
Mg	820.14	820.14	2.65	10.00	5114.90
Ca	247.18	12.00	0.80	30.00	1420.45
CO_3	0.00	0.00	0.00	61.86	0.00
HCO_3	402.49	402.49	2.68	2.68	531.22
SO_4	1724.45	1724.45	5.58	5.58	10754.78
Cl	58183.79	58219.24	248.22	248.22	62782.15
TDS	92593.13	92663.85	401.60	500.00	116062.71

These cost improvements can be seen in Table 21, where the total annualized costs for both the seawater feeds are presented along with the cost breakdown. The total costs for typical seawater decrease from 0.45 \$/m^3 to 0.39 \$/m^3 and for eastern Mediterranean,

they decrease from 0.46 $/m^3 to 0.44 $/m^3. Furthermore, Table 21 also compares the new optimized costs with those from the EOP treatment case to present the improved revenue generation from the salt production processes. The costs for the EOP treatment case were obtained from Table 16 since the change in NF modelling has a minimal effect on the overall costs. This is due to the fact that NF membranes in the base case and EOP treatment design play a minimal role in the system performance due to the small feed flow.

Table 21 Cost breakdown and comparison between typical brine treatment and hybrid membrane optimization approach using approximate NF model from literature

Typical Seawater			
	EOP Salt production	Optimized salt production	% Difference
Membranes	RO-NF	RO-RO-NF	
Total Cost ($/m^3)	0.47	0.39	16.08
Desal. Operating ($/m^3	0.43	0.48	-12.03
Desal. Capital ($/m^3)	0.12	0.12	-5.52
SPP Operating ($/m^3)	0.15	0.15	-1.85
SPP Capital ($/m^3)	0.25	0.26	-1.85
Salt revenue ($/m^3)	0.48	0.62	29.56
Eastern Mediterranean			
	EOP Salt production	Optimized salt production	% Difference
Membranes	RO-NF	RO-RO-NF	
Total Cost ($/m^3)	0.51	0.44	13.33
Desal. Operating ($/m^3	0.47	0.53	-11.45
Desal. Capital ($/m^3)	0.12	0.13	-5.81
SPP Operating ($/m^3)	0.15	0.15	-0.61
SPP Capital ($/m^3)	0.25	0.26	-0.61
Salt revenue ($/m^3)	0.49	0.62	26.83

9. CONCLUDING REMARKS

This work attempts to integrate two different aspects of membrane desalination research: membrane network superstructure optimization and salt production from desalination brines. Membrane network optimization of two different types of membranes such as RO and NF with their own set of connections within a superstructure was implemented for the first time. The contribution of NF membranes in channeling monovalent or divalent ions to certain SPPs was explored. Synthesis steps for superstructures consisting of both RO, NF membranes and SPPs were developed. The mathematical formulation to model this superstructure was also explained.

Proposed methodology was illustrated in a case study. Three membrane superstructures were designed with two SPPs producing $CaCO_3$ and NaCl. Approximate models for the SPPs and NF membrane were developed using literature and simulation data. The least cost membrane and SPP designs were obtained for two different seawater feeds. From the results, it was observed that the optimized design with salt production consists of two RO membranes and one NF membrane. Furthermore, this designs led to more than 20% reduction in total annualized costs when compared to the base case of desalination without salt production. The change in the total plant costs with salt prices was also analyzed.

The case study developed in this work used 2 SPPs producing only 2 salts. Future work in this area can develop models for different SPPs producing various other salts of higher value than $CaCO_3$ and NaCl to increase the product water discount. The formulation developed in this work assumes constant pressure for both RO and NF

membranes. NF performance models that are a function of both pressure and feed concentration can be used, thus allowing the feed pressures to be variables in the formulation. Several types of NF membranes, each with their different rejections for monovalent and divalent ions, exist and hence future work could implement this work's formulation with other NF membranes.

REFERENCES

1. IDE Technologies. What is Desalination. http://www.ide-tech.com/desalination/. Accessed January 1, 2015.
2. Morillo J, Usero J, Rosado D, El Bakouri H, Riaza A, Bernaola FJ. Comparative study of brine management technologies for desalination plants. *Desalination*. 2014;336(1):32-49. doi:10.1016/j.desal.2013.12.038.
3. Zhou D, Zhu L, Fu Y, Zhu M, Xue L. Development of lower cost seawater desalination processes using nano fi ltration technologies — A review. *Desalination*. 2015;376(1219):109-116. doi:10.1016/j.desal.2015.08.020.
4. Cooley H, Ajami N, Heberger M. *Key Issues in Seawater Desalination in California: Marine Impacts*. California; 2013. www.pacinst.org/publication/desal-marine-impacts.
5. Pérez-González A, Urtiaga AM, Ibáñez R, Ortiz I. State of the art and review on the treatment technologies of water reverse osmosis concentrates. *Water Res*. 2012;46(2):267-283. doi:10.1016/j.watres.2011.10.046.
6. Alnouri SY, Linke P. A systematic approach to optimal membrane network synthesis for seawater desalination. *J Memb Sci*. 2012;417-418:96-112. doi:10.1016/j.memsci.2012.06.017.
7. El-halwagi MM. Synthesis of Reverse-Osmosis Networks for Waste Reduction. *AIChE J*. 1992;38(8):1185-1198. doi:10.1002/aic.690380806.
8. Voros N, Maroulis ZB, Marinos-Kouris D. Optimization of reverse osmosis

networks for seawater desalination. *Comput Chem Eng*. 1996;20(96):S345-S350. doi:10.1016/0098-1354(96)00068-3.

9. Maskan F, Wiley DE, Johnston LPM, Clements DJ. Optimal design of reverse osmosis module networks. *AIChE J*. 2000;46(5):946-954. doi:10.1002/aic.690460509.

10. Zhu M, El-Halwagi MM, Al-Ahmad M. Optimal design and scheduling of flexible reverse osmosis networks. *J Memb Sci*. 1997;129(2):161-174. doi:10.1016/S0376-7388(96)00310-9.

11. Lu YY, Hu YD, Zhang XL, Wu LY, Liu QZ. Optimum design of reverse osmosis system under different feed concentration and product specification. *J Memb Sci*. 2007;287(2):219-229. doi:10.1016/j.memsci.2006.10.037.

12. Vince F, Marechal F, Aoustin E, Bréant P. Multi-objective optimization of RO desalination plants. *Desalination*. 2008;222(1-3):96-118. doi:10.1016/j.desal.2007.02.064.

13. Guria C, Bhattacharya PK, Gupta SK. Multi-objective optimization of reverse osmosis desalination units using different adaptations of the non-dominated sorting genetic algorithm (NSGA). *Comput Chem Eng*. 2005;29(9):1977-1995. doi:10.1016/j.compchemeng.2005.05.002.

14. Saif Y, Elkamel A, Pritzker M. Optimal design of reverse-osmosis networks for wastewater treatment. *Chem Eng Process Process Intensif*. 2008;47(12):2163-2174. doi:10.1016/j.cep.2007.11.007.

15. Marcovecchio MG, Aguirre P a., Scenna NJ. Global optimal design of reverse

osmosis networks for seawater desalination: Modeling and algorithm. *Desalination*. 2005;184(1-3):259-271. doi:10.1016/j.desal.2005.03.056.

16. Marriott J, Sørensen E. The optimal design of membrane systems. *Chem Eng Sci*. 2003;58(22):4991-5004. doi:10.1016/j.ces.2003.07.011.
17. Saif Y, Elkamel A, Pritzker M. Global optimization of reverse osmosis network for wastewater treatment and minimization. *Ind Eng Chem Res*. 2008;47(9):3060-3070. doi:10.1021/ie071316j.
18. Alnouri SY, Linke P. Optimal SWRO desalination network synthesis using multiple water quality parameters. *J Memb Sci*. 2013;444:493-512. doi:10.1016/j.memsci.2013.04.066.
19. Alnouri SY, Linke P. Optimal seawater reverse osmosis network design considering product water boron specifications. *Desalination*. 2014;345:112-127. doi:10.1016/j.desal.2014.04.030.
20. ICIS. Indicative Chemical Prices A-Z. http://www.icis.com/chemicals/channel-info-chemicals-a-z/. Accessed January 1, 2015.
21. Mundi I. Lime Prices In The United States, By Type. http://www.indexmundi.com/en/commodities/minerals/lime/lime_t5.html. Accessed January 1, 2015.
22. Co.Ltd DSGM. Potassium Sulphate/KMS. http://www.stargracemining.cn/productgrouplist-801233984/Potassium_Sulphate_KMS.html. Accessed August 25, 2015.
23. Motaung S, Maree J, De Beer M, Bologo L, Theron D, Baloyi J. Recovery of

Drinking Water and By-products from Gold Mine Effluents. *Int J Water Resour Dev*. 2008;24(3):433-450. doi:10.1080/07900620802150475.

24. Abboud NE, Chaaban FB, Tabanji WE. Economic evaluation of alternatives to reduce SO_2 emissions from power plants. *Int J Environ Stud*. 2000;57(2):225-238. doi:10.1080/00207230008711268.

25. Katzir L, Volkmann Y, Daltrophe N, et al. WAIV - Wind aided intensified evaporation for brine volume reduction and generating mineral byproducts. *Desalin Water Treat*. 2010;13(1-3):63-73. doi:10.5004/dwt.2010.772.

26. Gilron J, Folkman Y, Savliev R, Waisman M, Kedem O. WAIV - Wind aided intensified evaporation for reduction of desalination brine volume. *Desalination*. 2003;158(1-3):205-214. doi:10.1016/S0011-9164(03)00453-3.

27. GEA. *Mass Crystallization from Solutions*. Neatherlands; 2010. http://www.gea.com/global/en/binaries/2010-03_Mass crystallization from solutions_sm_tcm11-21834.pdf.

28. Zarzo Martinez D, Campos Pozuelo E. Project for the development of innovative solutions for brines from desalination plants. *Desalin Water Treat*. 2011;31(1-3):206-217. doi:10.5004/dwt.2011.2371.

29. Mickley M. *Survery of High-Recovery and Zero Liquid Discharge Technologies for Water Utilities*. Alexandria; 2007. http://www.waterboards.ca.gov/water_issues/programs/grants_loans/water_recycling/research/02_006a_01.pdf.

30. Gabelich CJ, Rahardianto A, Northrup CR, Yun TI, Cohen Y. Process evaluation

of intermediate chemical demineralization for water recovery enhancement in production-scale brackish water desalting. *Desalination*. 2011;272(1-3):36-45. doi:10.1016/j.desal.2010.12.050.

31. Rahardianto A, Gao J, Gabelich CJ, Williams MD, Cohen Y. High recovery membrane desalting of low-salinity brackish water: Integration of accelerated precipitation softening with membrane RO. *J Memb Sci*. 2007;289(1-2):123-137. doi:10.1016/j.memsci.2006.11.043.

32. Ahmed M, Arakel A, Hoey D, et al. Feasibility of salt production from inland RO desalination plant reject brine: A case study. *Desalination*. 2003;158(1-3):109-117. doi:10.1016/S0011-9164(03)00441-7.

33. Stepakoff GL, Siegelman D, Johnson R, Gibson W. Development of a eutectic freezing process for brine disposal. *Desalination*. 1974;15(1):25-38. doi:10.1016/S0011-9164(00)82061-5.

34. Himawan C, Kramer HJM, Witkamp GJ. Study on the recovery of purified MgSO4·7H2O crystals from industrial solution by eutectic freezing. *Sep Purif Technol*. 2006;50(2):240-248. doi:10.1016/j.seppur.2005.11.031.

35. Drioli E, Curcio E, Criscuoli A, Di Profio G Di. Integrated system for recovery of CaCO3, NaCl and MgSO 4·7H2O from nanofiltration retentate. *J Memb Sci*. 2004;239(1):27-38. doi:10.1016/j.memsci.2003.09.028.

36. Badruzzaman M, Oppenheimer J, Adham S, Kumar M. Innovative beneficial reuse of reverse osmosis concentrate using bipolar membrane electrodialysis and electrochlorination processes. *J Memb Sci*. 2009;326(2):392-399.

doi:10.1016/j.memsci.2008.10.018.

37. Drioli E, Curcio E, Di Profio G, Macedonio F, Criscuoli A. Integrating Membrane Contactors Technology and Pressure-Driven Membrane Operations for Seawater Desalination. *Chem Eng Res Des*. 2006;84(3):209-220. doi:10.1205/cherd.05171.

38. El-Said GF, Moneer AA, El-Sadaawy MM, Morsy AMH, Shaltout NA. The precipitation of fluoride, calcium and magnesium minerals from Egyptian Mediterranean Sea coast in relation to discharged waters. *Desalin Water Treat*. 2016;57(5):2113-2124. doi:10.1080/19443994.2014.979243.

39. Wilf M. *The Guidebook to Membrane Desalination Technology*. Balaban Desalination Publications; 2007.

40. Kaya C, Sert G, Kabay N, Arda M, Yüksel M, Egemen Ö. Pre-treatment with nanofiltration (NF) in seawater desalination—Preliminary integrated membrane tests in Urla, Turkey. *Desalination*. 2015;369:10-17. doi:10.1016/j.desal.2015.04.029.

41. Dow Water & Process Solutions. *FILMTEC Reverse Osmosis Membranes - Technical Manual*.; 2015. http://msdssearch.dow.com/PublishedLiteratureDOWCOM/dh_095b/0901b8038095b91d.pdf?filepath=liquidseps/pdfs/noreg/609-00071.pdf&fromPage=GetDoc.

42. Al-Zoubi H, Hilal N, Darwish N a., Mohammad a. W. Rejection and modelling of sulphate and potassium salts by nanofiltration membranes: neural network and Spiegler-Kedem model. *Desalination*. 2007;206(1-3):42-60. doi:10.1016/j.desal.2006.02.060.

43. Fridman-Bishop N, Nir O, Lahav O, Freger V. Predicting the Rejection of Major Seawater Ions by Spiral-Wound Nanofiltration Membranes. *Environ Sci Technol*. 2015;49(14):8631-8638. doi:10.1021/acs.est.5b00336.

44. Pérez-González A, Ibáñez R, Gómez P, Urtiaga a. M, Ortiz I, Irabien J a. Nanofiltration separation of polyvalent and monovalent anions in desalination brines. *J Memb Sci*. 2015;473:16-27. doi:10.1016/j.memsci.2014.08.045.

45. Dow Solutions - Water & Process. ROSA System Design Software. 2007. http://www.dow.com/en-us/water-and-process-solutions/resources/design-software.

46. Mabrouk AN a., Fath HES. Techno-economic analysis of hybrid high performance MSF desalination plant with NF membrane. *Desalin Water Treat*. 2012;(August 2015):1-13. doi:10.1080/19443994.2012.714893.

47. Ayoub GM, Zayyat RM, Al-Hindi M. Precipitation softening: A pretreatment process for seawater desalination. *Environ Sci Pollut Res*. 2014;21(4):2876-2887. doi:10.1007/s11356-013-2237-1.

48. Aguinaldo JT. Application of integrated chemical precipitation and ultrafiltration as pre-treatment in seawater desalination. *Desalin Water Treat*. 2009;2(1-3):113-125. doi:10.5004/dwt.2009.163.

49. Mohammadesmaeili F, Badr MK, Abbaszadegan M, Fox P. Byproduct recovery from reclaimed water reverse osmosis concentrate using lime and soda-ash treatment. *Water Environ Res*. 2010;82(4):342-350. doi:10.2175/106143009X12487095236919.

50. Monroe Environmental. *Circular Clarifiers*. http://www.monroeenvironmental.com/water-and-wastewater-treatment/circular-clarifiers/circular-clarifiers-clean-water.

51. Sorour MH, Hani HA, Shaalan HF, Al-Bazedi GA. Preliminary techno-economics assessment of developed desalination/salt recovery facility based on membrane and thermal techniques. *Desalin Water Treat*. 2014;3994(January):1-7. doi:10.1080/19443994.2014.947775.

52. United States Geological Survey. PHREEQC. 1998. http://wwwbrr.cr.usgs.gov/projects/GWC_coupled/phreeqc/.

53. Davis M, Cornwell D. *Introduction to Environmental Engineering*. 5th ed. McGraw-Hill Series in Civil and Environmental Engineering

54. Ericsson B, Hallmans B. Treatment of saline wastewater for zero discharge at the Debiensko coal mines in Poland. *Desalination*. 1996;105(1-2):115-123. doi:10.1016/0011-9164(96)00065-3.

55. Lozier JC, Hwang M, Williams R. Ro concentrate treatment and reuse to achieve sustainable water management schemes for industrial facilities located in arid, water scarce regions. *AMTA/AWWA Membr Technol Conf Expo 2013*. 2013:1266-1280. http://www.scopus.com/inward/record.url?eid=2-s2.0-84890334614&partnerID=tZOtx3y1.

56. Bazedi G Al, Ettouney R. Salt recovery from brine generated by large-scale seawater desalination plants. *Desalin Water Treat*. 2013;52(25-27):4689-4697. doi:10.1080/19443994.2013.810381.

57. Farahbod F, Mowla D, Nasr MRJ, Soltanieh M. Experimental study of forced circulation evaporator in zero discharge desalination process. *Desalination*. 2012;285:352-358. doi:10.1016/j.desal.2011.10.026.

58. Ludwig H. *COMPOSITION OF DESALINATED WATER*. Vol II. http://www.desware.net/Sample-Chapters/D02/13-002.pdf.

59. World's Richest Countries. Top Salt Importers 2014. http://www.worldsrichestcountries.com/top-salt-importers.html. Accessed January 1, 2015.

60. Kelting DL, Laxson CL. Review of Effects and Costs of Road De-icing with Recommendations for Winter Road Management in the Adirondack Park. *AdkAction.org*. 2010;(February).

61. Peters M, Timmerhaus K, West R. *Plant Design and Economics for Chemical Engineers*. 5th ed. McGraw-Hill; 2003.

62. Macedonio F, Curcio E, Drioli E. Integrated membrane systems for seawater desalination: energetic and exergetic analysis, economic evaluation, experimental study. *Desalination*. 2007;203(1-3):260-276. doi:10.1016/j.desal.2006.02.021.

63. Haddad Z. Solvay Chemicals increases its prices for soda ash. http://www.solvay.us/en/media/press_releases/Soda-Ash-2015-Price- Increase-07-20-15.html. Published 2015. Accessed January 1, 2015.

64. Smith MK, Newell TA. Simulation and economic evaluation of a solar evaporation system for concentrating sodium chloride brines. *Sol Energy*. 1991;46(6):389-399.

65. Sagie D, Feinerman E, Aharoni E. Potential of solar desalination in Israel and in its

close vicinity. *Desalination*. 2001;139(1-3):21-33. doi:10.1016/S0011-9164(01)00291-0.

66. Subramani A, Jacangelo JG. Treatment technologies for reverse osmosis concentrate volume minimization: A review. *Sep Purif Technol*. 2014;122:472-489. doi:10.1016/j.seppur.2013.12.004.

APPENDIX

Table 22 General formulation expressions that determine the initial and final pressures of each type of stream connection.

Initial Pressure Specification	Final pressure specification	Conditions
$PI_{j,j'}^{PRO-RO} = P_j^{P-RO}$	$PF_{j,j'}^{PRO-RO} = P_{j'}^{F-RO}$	$j, j' \in J, j \neq j'$
$PI_{j,j'}^{PRO-NF} = P_j^{P-RO}$	$PF_{j,j'}^{PRO-NF} = P_{j'}^{F-NF}$	$j, j' \in J, j \neq j'$
$PI_{j,j'}^{PNF-RO} = P_j^{P-NF}$	$PF_{j,j'}^{PNF-RO} = P_{j'}^{F-RO}$	$j, j' \in J, j \neq j'$
$PI_{j,j'}^{PNF-NF} = P_j^{P-NF}$	$PF_{j,j'}^{PNF-NF} = P_{j'}^{F-NF}$	$j, j' \in J, j \neq j'$
$PI_{j,j'}^{BRO-RO} = P_j^{B-RO}$	$PF_{j,j'}^{BRO-RO} = P_{j'}^{F-RO}$	$j, j' \in J, j \neq j'$
$PI_{j,j'}^{BRO-NF} = P_j^{B-RO}$	$PF_{j,j'}^{BRO-NF} = P_{j'}^{F-NF}$	$j, j' \in J, j \neq j'$
$PI_{j,j'}^{BNF-RO} = P_j^{B-NF}$	$PF_{j,j'}^{BNF-RO} = P_{j'}^{F-RO}$	$j, j' \in J, j \neq j'$
$PI_j^{PRO-PROD} = P_j^{P-RO}$	$PF_j^{PNF-PROD} = P^{PROD}$	$j \in J$
$PI_j^{PNF-PROD} = P_j^{P-NF}$	$PF_j^{PNF-PROD} = P^{PROD}$	$j \in J$
$PI_j^{BRO-BRINE} = P_j^{B-RO}$	$PF_j^{BRO-BRINE} = P^{BRINE}$	$j \in J$
$PI_j^{PNF-BRINE} = P_j^{P-NF}$	$PF_j^{PNF-BRINE} = P^{BRINE}$	$j \in J$
$PI_j^{BNF-BRINE} = P_j^{B-NF}$	$PF_j^{BNF-BRINE} = P^{BRINE}$	$j \in J$
$PI_{j,s}^{BRO-S} = P_j^{B-RO}$	$PF_{j,s}^{BRO-S} = P_s^{F-S}$	$j \in J, s \in S$
$PI_{j,s}^{BNF-S} = P_j^{B-NF}$	$PF_{j,s}^{BNF-S} = P_s^{F-S}$	$j \in J, s \in S$
$PI_{j,s}^{PNF-S} = P_j^{P-NF}$	$PF_{j,s}^{PNF-S} = P_s^{F-S}$	$j \in J, s \in S$
$PI_{s,j}^{S-RO} = P_s^{S-Br}$	$PF_{s,j}^{S-RO} = P_j^{F-RO}$	$s \in S, j \in J$
$PI_{s,j}^{S-NF} = P_s^{S-Br}$	$PF_{s,j}^{S-NF} = P_j^{F-NF}$	$s \in S, j \in J$
$PI_{s,s'}^{S-S} = P_s^{S-Br}$	$PI_{s,s'}^{S-S} = P_s^{F-S}$	$s, s' \in S, s \neq s'$
$PI_s^{S-PROD} = P_s^{S-Re}$	$PF_s^{S-PROD} = P^{PROD}$	$s \in S$
$PI_s^{S-BRINE} = P_s^{S-Br}$	$PF_s^{S-BRINE} = P^{BRINE}$	$s \in S$

Table 23 RO membrane modelling equations

Total Number of RO Membrane Modules (per system Stage/Pass)	$= \frac{NM_j^{RO}}{19000 F_j^{F-RO}}$ $3.28^2 SM_j \bar{A}(\bar{\pi})_j (TCF_j)(FF_j) P_j^{F-RO} - \frac{\Delta P_{fc,j}}{2} P_j^{P-RO} - \pi_j^F \left(\left(\frac{C_{fc}}{C_f}\right)_j \times exp^{(0.7 \times R_j)} - (1 - R_j^{RO}) \right)$ j∈J
Membrane permeability as a function of average concentrate side osmotic pressure	$if\ \pi_j^F < 25, \quad \bar{A}(\bar{\pi})_j = 0.125$ $if\ 25 < \pi_j^F < 200, \quad \bar{A}(\bar{\pi})_j = 0.125 - 0.011 \left(\frac{(\pi_j^F - 25)}{35} \right)$ j∈J $if\ \pi_j^F > 200, \quad \bar{A}(\bar{\pi})_j = 0.07 - 0.0001(\pi_j^F - 200)$ j∈J
Temperature correction factor	$if\ T \geq 25, \quad TCF_j = exp^{2460 \times \left(\frac{1}{298} - \frac{1}{273+T}\right)}$ $if\ T \leq 25, \quad TCF_j = exp^{3020 \times \left(\frac{1}{298} - \frac{1}{273+T}\right)}$
Average concentrate side system pressure drop	$\Delta P_{fc,j} = (6.8948 \times 10^{-2})(0.04) \left(13.2 \frac{(F_j^{F-RO} + F_j^{B-RO})}{2} \right)^2$ j∈J
Log mean concentrate-side to feed concentration ratio	$\left(\frac{C_{fc}}{C_f}\right)_j = \frac{-\ln(1 - R_j)}{R_j}$ j∈J
Membrane feed stream osmotic pressure (Total & Component)	$\pi_{i,j}^F = (6.8948 \times 10^{-2}) \frac{1.12(273+T) F_j^F X_{i,j}^F}{39102}$ i∈I and j∈J $\pi_j^F = \sum_{i=1}^{Nc} \pi_{i,j}^F$ j∈J

Table 24 Membrane network cost equations

Total Capital Investment for membrane network	$TCI_{Membrane} = (DDC_{Membrane} + SC_{Membrane} + CC_{contingency-membrane})/L$
Direct Capital Costs for membrane network	$DDC_{Membrane} = CC_{Site\ Preparation} + CC_{Intake} + CC_{Pretreatment} + CC_{RO\ System} + CC_{Post\ treatment} + CC_{Waste\ disposal/Cleaning} + CC_{Inst\ \&\ Control} + CC_{Buildings} + CC_{Electrical} + CC_{Startup} + CC_{BTP}$
Site Preparation	$CC_{Site\ Preparation} = 432 \times F^{FEED} \times \alpha_{sc}$
Intake	$CC_{Intake} = 1963.6 \times F^{FEED} \times \alpha_{sc}$
Pretreatment	$CC_{Pretreatment} = 2700 \times F^{FEED} \times \alpha_{sc}$
Membrane System	$CC_{RO\ System} = CC_{Skids} + CC_{Piping} + CC_{cartridge\ filters} + CC_{modules} + CC_{Pumps} + CC_{ERDs}$
Membrane Skids	$CC_{Skids} = 250000 \times NM_j$
Membrane piping	$CC_{Piping} = 1369.61 \times \frac{F^{PROD}}{F^{PROD}/F^{FEED}} \times \alpha_{sc}$
Membrane Cartridge Filters	$CC_{cartridge\ filters} = 112836 \times \left(\frac{F^{FEED} \times 86.4}{3600 \times 24/NS}\right)^{0.831} \times NS \times 1.2 \times \alpha_{sc}$
Modules	$CC_{modules} = \sum_{j=1}^{Nm} 5000 \times NM_j^{RO} \times y_j^{RO} + \sum_{j=1}^{Nm} 3222 \times NM_j^{NF} \times y_j^{NF}$
Membrane Pumps	$CC_{pumps} = 58000 \times (PW^{Pumps} \times 0.0134)^{0.65}; if\ PW^{Pumps} < 224\ kW,$ $C_{pumps} = 50000 + 234.5 \times PW^{Pumps}; if\ PW^{Pumps} > 224\ kW$
Membrane Energy Recovery Devices	$CC_{ERDs} = 85000 \times \left(PW^{ERDs} \times \frac{1.34}{100}\right)^{0.65}; if\ PW^{ERDs} < 373$ hp $CC_{ERDs} = 0.378 \times (PW^{ERDs} \times 1.34)^{0.81} \times 1000;\ if\ PW^{ERDs} > 373$ hp,
Post Treatment	$CC_{Post\ treatment} = 785.45 \times F^{FEED} \times \alpha_{sc}$
Waste Disposal & Cleaning	$CC_{Waste\ disposal/Cleaning} = CC_{Membrane\ Cleaning} + CC_{Solids} + CC_{concentrate\ stream\ disposal}$
Membrane Cleaning Chemicals	$CC_{Membrane\ Cleaning} = 432 \times F^{FEED} \times \alpha_{sc}$
Solids	$CC_{Solids} = 432 \times F^{FEED} \times \alpha_{sc}$
Concentrate Stream Disposal	$CC_{concentrate\ stream\ disposal} = 1296 \times F^{FEED} \times \alpha_{sc}$
Instrumentation & Control	$CC_{Inst\ \&\ Control} = 300000 + 65000 \times NS$

Table 24 - Continued

Buildings	$CC_{Buildings} = ((-10^{-6} \times (86.4 \times F^{PROD})^2 + 0.3668^{86.4 \times F^{PROD}} + 1887.9 \times 5 + 1728 \times F^{FEED}) \times \alpha_{sc}$
Electrical	$CC_{Electrical} = 614 \times (F^{PROD} \times 86.4)^{0.65} \times \alpha_{sc}$
Auxiliary Service Equipment	$CC_{Aux\ Service\ Eqp} = 785.45 \times F^{FEED} \times \alpha_{sc}$
Startup, Commission & Acceptance	$CC_{Startup} = 785.45 \times F^{FEED} \times \alpha_{sc}$
Soft Costs	$SC = CC_{Project\ services} + CC_{Project\ development} + CC_{Project\ financing}$
Project Engineering Services	$CC_{Project\ services} = 2304 \times F^{FEED} \times \alpha_{sc}$
Project Development	$CC_{Project\ development} = 1944 \times F^{FEED} \times \alpha_{sc}$
Project Financing	$CC_{Project\ financing} = 0.04\ DCC$
Contingency	$CC_{contingency} = 0.05(DCC + SC)$
Total Operating Costs for membrane network	$TOC_{Membrane} = VOC_{Membrane} + FOC_{Membrane}$
Variable Operating & Maintenance (O&M) Costs	$VOC_{Membrane} = OC_{Power} + OC_{chemicals} + OC_{Membrane\ replacement} + OC_{Filter\ replacement} + OC_{Waste\ stream\ disposal} + OC_{BTP}$
Power Costs	$OC_{Power} = OC_{Intake} + OC_{Pretreatment} + OC_{RO} + OC_{Post\ treamtent} + OC_{Membrane\ cleaning} + OC_{Service\ facilities}$
Intake	$OC_{Intake} = \frac{0.191 \times (PW^{Pumps} - PW^{ERDs}) \times 24 \times PWC \times 365 \times \alpha_{sc}}{3.38}$
Pretreatment	$OC_{Pretreatment} = \frac{0.013 \times (PW^{Pumps} - PW^{ERDs}) \times 24 \times PWC \times 365 \times \alpha_{sc}}{3.38}$
Reverse Osmosis	$OC_{RO} = (PW^{Pumps} - PW^{ERDs}) \times PWC \times 365 \times 24$
Post Treatment	$OC_{Post\ treamtent} = \frac{0.177 \times (PW^{Pumps} - PW^{ERDs}) \times 24 \times PWC \times 365 \times \alpha_{sc}}{3.38}$
Membrane Cleaning	$OC_{Membrane\ cleaning} = \frac{0.027 \times (PW^{Pumps} - PW^{ERDs}) \times 24 \times PWC \times 365 \times \alpha_{sc}}{3.38}$
Service Facilities	$OC_{Service\ facilities} = \frac{0.13 \times (PW^{Pumps} - PW^{ERDs}) \times 24 \times PWC \times 365 \times \alpha_{sc}}{3.38}$
Chemicals	$OC_{Chemicals} = 378.4 \times F^{FEED} \times \alpha_{sc}$

Table 24 - Continued

Membrane Replacement	$OC_{Membrane\ replacement} = \sum_{j=1}^{Nro} 2.5 \times SM_j \times NM_j \times \alpha_{sc}$
Cartridge Filter Replacement	$OC_{Filter\ replacement} = 23.097 \times F^{FEED} \times NS \times 2.94 \times \alpha_{sc}$
Waste Stream Disposal	$OC_{Waste\ stream\ disposal} = 315.36 \times F^{FEED} \times \alpha_{sc}$
Fixed Operating & Maintenance Costs	$FOC_{Membrane} = OC_{Labor} + OC_{Manitenance} + OC_{Env.\ \&\ Monitoring} + OC_{Indirect\ O\&M}$
Labor	$OC_{Labor} = 378.43 \times F^{FEED} \times \alpha_{sc}$
Maintenance	$OC_{Manitenance} = 630.72 \times F^{FEED} \times \alpha_{sc}$
Environmental & Performance Monitoring	$OC_{Env.\ \&\ Monitoring} = 50.46 \times F^{FEED} \times \alpha_{sc}$
Indirect O&M	$OC_{Indirect\ O\&M} = 756.86 \times F^{FEED} \times \alpha_{sc}$
Power Requirements, Pumps	$PW^{Pumps} = 1.34(\sum_{j,j\prime=1}^{Nm} z_{j,j\prime}^{PRO-RO} PW_{j,j\prime}^{PRO-RO} + \sum_{j,j\prime=1}^{Nm} z_{j,j\prime}^{PRO-NF} PW_{j,j\prime}^{PRO-NF} + \sum_{j\prime=1}^{Nm} z_{j\prime}^{FEED-RO} PW_{j\prime}^{FEED-RO} + \sum_{j\prime=1}^{Nm} z_{j\prime}^{FEED-NF} PW_{j\prime}^{FEED-NF} + \sum_{j,j\prime=1}^{Nm} z_{j,j\prime}^{PNF-RO} PW_{j,j\prime}^{PNF-RO} + \sum_{j,j\prime=1}^{Nm} z_{j,j\prime}^{PNF-NF} PW_{j,j\prime}^{PNF-NF} + \sum_{j,j\prime=1}^{Nm} z_{j,j\prime}^{BNF-RO} PW_{j,j\prime}^{BNF-RO} + \sum_{j,j\prime=1}^{Nm} z_{j,j\prime}^{BRO-NF} PW_{j,j\prime}^{BRO-NF} + \sum_{j,j\prime=1}^{Nm} z_{j,j\prime}^{BNF-NF} PW_{j,j\prime}^{BNF-NF})$
Power Recovery, ERDs	$PW^{ERDs} = 1.34(\sum_{j=1}^{Nm} z_j^{BRO-BRINE} PW_j^{BRO-BRINE} + \sum_{j,j\prime=1}^{Nm} z_{j,j\prime}^{BRO-NF} PW_{j,j\prime}^{BRO-NF} + \sum_{j,s=1}^{Nm} z_{j,s}^{BRO-S} PW_{j,s}^{BRO-S} + \sum_{j,s=1}^{Nm} z_{j,s}^{PNF-S} PW_{j,s}^{PNF-S} + \sum_{j=1}^{Nm} z_j^{BNF-BRINE} PW_j^{BNF-BRINE} + \sum_{j,s=1}^{Nm} z_{j,s}^{BNF-S} PW_{j,s}^{BNF-S}$